AD-A174 606 A NUMERICAL INVESTIGATION OF ASTRONOMIC TIDAL 1/1
CIRCULATION IN PUGET SOUND(U) COASTAL ENGINEERING
RESEARCH CENTER VICKSBURG MS R A SCHMALZ SEP 86

UNCLASSIFIED CERC-MP-86-9 F/G 8/3 NL

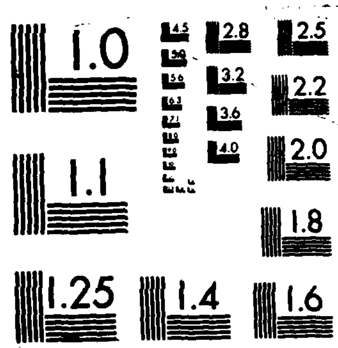

CROCOPY RESOLUTION TEST CHART

US Army Corps of Engineers

AD-A174 606

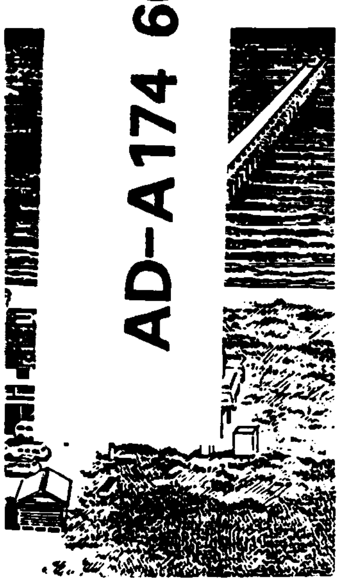

(2)

MISCELLANEOUS PAPER CERC-86-9

A NUMERICAL INVESTIGATION OF ASTRONOMIC TIDAL CIRCULATION IN PUGET SOUND

by

Richard A. Schmalz, Jr.

Coastal Engineering Research Center

DEPARTMENT OF THE ARMY
Waterways Experiment Station, Corps of Engineers
PO Box 631, Vicksburg, Mississippi 39180-0631

US ARMY ENGINEER WATERWAYS EXPERIMENT STATION

September 1986
Final Report

Approved For Public Release; Distribution Unlimited

Prepared for US Army Engineer District, Seattle
PO Box C-3755, Seattle, Washington, DC 98124-2255

COASTAL ENGINEERING RESEARCH CENTER

Unclassified
SECURITY CLASSIFICATION OF THIS PAGE

AD-A174 666

REPORT DOCUMENTATION PAGE

Form Approved
OMB No 0704-0188
Exp Date Jun 30, 1986

1a REPORT SECURITY CLASSIFICATION: Unclassified

1b RESTRICTIVE MARKINGS:

2a SECURITY CLASSIFICATION AUTHORITY:

2b DECLASSIFICATION/DOWNGRADING SCHEDULE:

3 DISTRIBUTION/AVAILABILITY OF REPORT: Approved for public release; distribution unlimited

4 PERFORMING ORGANIZATION REPORT NUMBER(S): Miscellaneous Paper CERC-86-9

5 MONITORING ORGANIZATION REPORT NUMBER(S):

6a NAME OF PERFORMING ORGANIZATION: USAEWES, Coastal Engineering Research Center

6b OFFICE SYMBOL (If applicable): WESCV

7a NAME OF MONITORING ORGANIZATION:

6c ADDRESS (City, State, and ZIP Code): PO Box 631, Vicksburg, MS 39180-0631

7b ADDRESS (City, State, and ZIP Code):

8a NAME OF FUNDING/SPONSORING ORGANIZATION: USAE District, Seattle

8b OFFICE SYMBOL (If applicable):

9 PROCUREMENT INSTRUMENT IDENTIFICATION NUMBER:

8c ADDRESS (City, State, and ZIP Code): PO Box C-3755, Seattle, WA 98124-2255

10 SOURCE OF FUNDING NUMBERS

PROGRAM ELEMENT NO	PROJECT NO	TASK NO	WORK UNIT ACCESSION NO

11 TITLE (Include Security Classification): A Numerical Investigation of Astronomic Tidal Circulation in Puget Sound

12 PERSONAL AUTHOR(S): Schmalz, Richard A.

13a TYPE OF REPORT: Final report

13b TIME COVERED: FROM Jul 85 TO Jan 86

14 DATE OF REPORT (Year, Month, Day): September 1986

15 PAGE COUNT: 62

16 SUPPLEMENTARY NOTATION: Available from National Technical Information Service, 5285 Port Royal Road, Springfield, VA 22161.

17 COSATI CODES

FIELD	GROUP	SUB-GROUP

18 SUBJECT TERMS (Continue on reverse if necessary and identify by block number):
Finite difference method
Hydrodynamics
Mathematical models
Puget sound
Dredge disposal

19 ABSTRACT (Continue on reverse if necessary and identify by block number)

The astronomic tidal circulation in Puget Sound, Washington, is investigated using the Waterways Implicit Flooding Model (WIFM) in a two-dimensional, vertically-averaged context. The state of knowledge of general circulation characteristics is presented as a prelude to the numerical modeling investigation. A general tide prediction program has been developed which predicts both tidal elevations and horizontal currents. Astronomic tidal characteristics are studied on a 70 (horizontal) by 103 (vertical) dimension global grid comprising 7,210 cells with a maximum spatial resolution of 3,750 ft. A 90-sec time-step was employed in all WIFM long-wave simulations resulting in a maximum Courant number of 4.1. Simulated tidal elevations and vertically-averaged currents were calibrated to predicted values for the 16-18 January 1981 spring tide period. Calibrated bottom friction mechanics were verified using the 13-15 January 1981 neap tide period. Simulated results corresponded to predicted values of elevation and current except for some discrepancies in

(Continued)

20 DISTRIBUTION/AVAILABILITY OF ABSTRACT: ☐ UNCLASSIFIED/UNLIMITED ☐ SAME AS RPT ☐ DTIC USERS

21 ABSTRACT SECURITY CLASSIFICATION: Unclassified

22a NAME OF RESPONSIBLE INDIVIDUAL:

22b TELEPHONE (Include Area Code):

22c OFFICE SYMBOL:

DD FORM 1473, 84 MAR

83 APR edition may be used until exhausted
All other editions are obsolete

SECURITY CLASSIFICATION OF THIS PAGE
Unclassified

20. ABSTRACT (Continued).

the Southern Basin. Peak current magnitudes were tabulated at existing disposal sites for both calibration and verification of astronomic tide conditions. Meteorological effects and freshwater inflows were not considered. The 11-13 December 1985 extreme spring tide period was also simulated, and maximum current velocities and their associated times of occurrence were tabulated.

PREFACE

A numerical investigation of astronomic tidal circulation was performed for Puget Sound. The general nature of the astronomic tidal circulation was investigated in qualitative terms for both Puget Sound and its approaches. A tide prediction program was developed also. Detailed numerical simulations employing a two-dimensional, vertically integrated model were performed to characterize maximum velocities at seven dredged material disposal sites under a range of conditions. The results of this investigation are reported herein.

Project administration and funding were provided by the US Army Engineer District, Seattle (NPS). Program development and computer simulation work were conducted by the US Army Engineer Waterways Experiment Station (WES) in the Coastal Processes Branch of the Coastal Engineering Research Center (CERC) during the period July 1985 through January 1986 under general supervision of Dr. James R. Houston and Mr. Charles C. Calhoun, Chief and Assistant Chief, CERC, respectively; and under direct supervision of Mr. H. Lee Butler, Chief Research Division (CR). This report was prepared by Dr. Richard A. Schmalz, Jr., CR, with assistance from Mses. Brenda O. Dee and Carolyn A. Hunt, CR, in developing the global grid and attendant data sets. Ms. Dee also assisted in developing PART II of the report.

Mr. Eric Nelson, NPS, is gratefully acknowledged for coordinating the numerical modeling efforts. Dr. Harold O. Mofjeld, Pacific Marine Environmental Laboratory (PMEL), is acknowledged for furnishing the harmonic constituents for the current compounds at selected stations. Dr. Mofjeld also provided helpful information on numerical modeling activities at PMEL as well as copies of several major studies conducted at PMEL and reprints of journal articles written by PMEL personnel. This report was edited by Ms. Shirley A. J. Hanshaw, Information Products Division, Information Technology Laboratory, WES.

Director of WES during the conduct of this study was COL Allen F. Grum, USA. Commander and Director of WES during report publication was COL Dwayne G. Lee, CE. Technical Director was Dr. Robert W. Whalin.

CONTENTS

Page

PREFACE 1

CONVERSION FACTORS, NON-SI TO SI (METRIC) UNITS OF MEASUREMENT 3

PART I: INTRODUCTION 4

PART II: GENERAL NATURE OF TIDAL CIRCULATION 6

PART III: TIDE PREDICTION PROGRAM 15

Tidal Elevation Determination 17
Tidal Current Analysis 20

PART IV: NUMERICAL LONG-WAVE INVESTIGATION 22

Puget Sound Global Grid Development 23
Calibration Period 29
Verification Period 33
Extreme Spring Tide Simulation Period 35

PART V: SUMMARY AND CONCLUSIONS 37

REFERENCES 39

PLATES 1-17

CONVERSION FACTORS, NON-SI TO SI (METRIC) UNITS OF MEASUREMENT

Non-SI units of measurement used in this report can be converted to SI (metric) units as follows:

Multiply	By	To Obtain
cubic feet per second	0.028317	cubic metres per second
cubic miles (nautical)	6.352	cubic kilometres
fathoms	1.8288	metres
feet	0.3048	metres
knots (international)	0.5144444	metres per second
square miles (nautical)	3.430	square kilometres

A NUMERICAL INVESTIGATION OF ASTRONOMIC TIDAL CIRCULATION IN PUGET SOUND

PART I: INTRODUCTION

1. The US Army Engineer District, Seattle (NPS), in conjunction with Region X, US Environmental Protection Agency, the State of Washington Department of Natural Resources, and the State of Washington Department of Ecology has initiated a 3-year two-phase study for preparation of an Environmental Impact Statement on dredge disposal within Puget Sound, Washington, waters. The goal of the Puget Sound Dredge Disposal Analysis (PSDDA) Program is to furnish the basis for environmentally effective plans for unconfined disposal of dredged material in Puget Sound. The Phase I effort will concern itself with Central Puget Sound, indicated in Figure 1. In Phase II (Figure 1), the remaining disposal areas will be considered.

2. As part of the Phase I effort, NPS provided funding for the Coastal Engineering Research Center (CERC) of the US Army Engineer Waterways Experiment Station (WES) to investigate the current structure in and around potential and existing disposal sites in the central sound. This report documents the results of this investigation in the context of a two-dimensional, vertically integrated modeling approach and is organized in the following manner. In Part II, the state of present knowledge on the general nature of circulation in Puget Sound is presented. In Part III, a general astronomic tidal elevation and current prediction program is developed and results presented for Puget Sound. Part IV details the numerical long-wave model application. The 16-18 January 1981 spring tide period is employed for model calibration, while the 13-15 January 1981 neap tide period is utilized as a verification period. Tidal current conditions are also investigated for the 11-13 December 1985 extreme spring tide condition. In Part V, major study results are summarized, and conclusions are drawn.

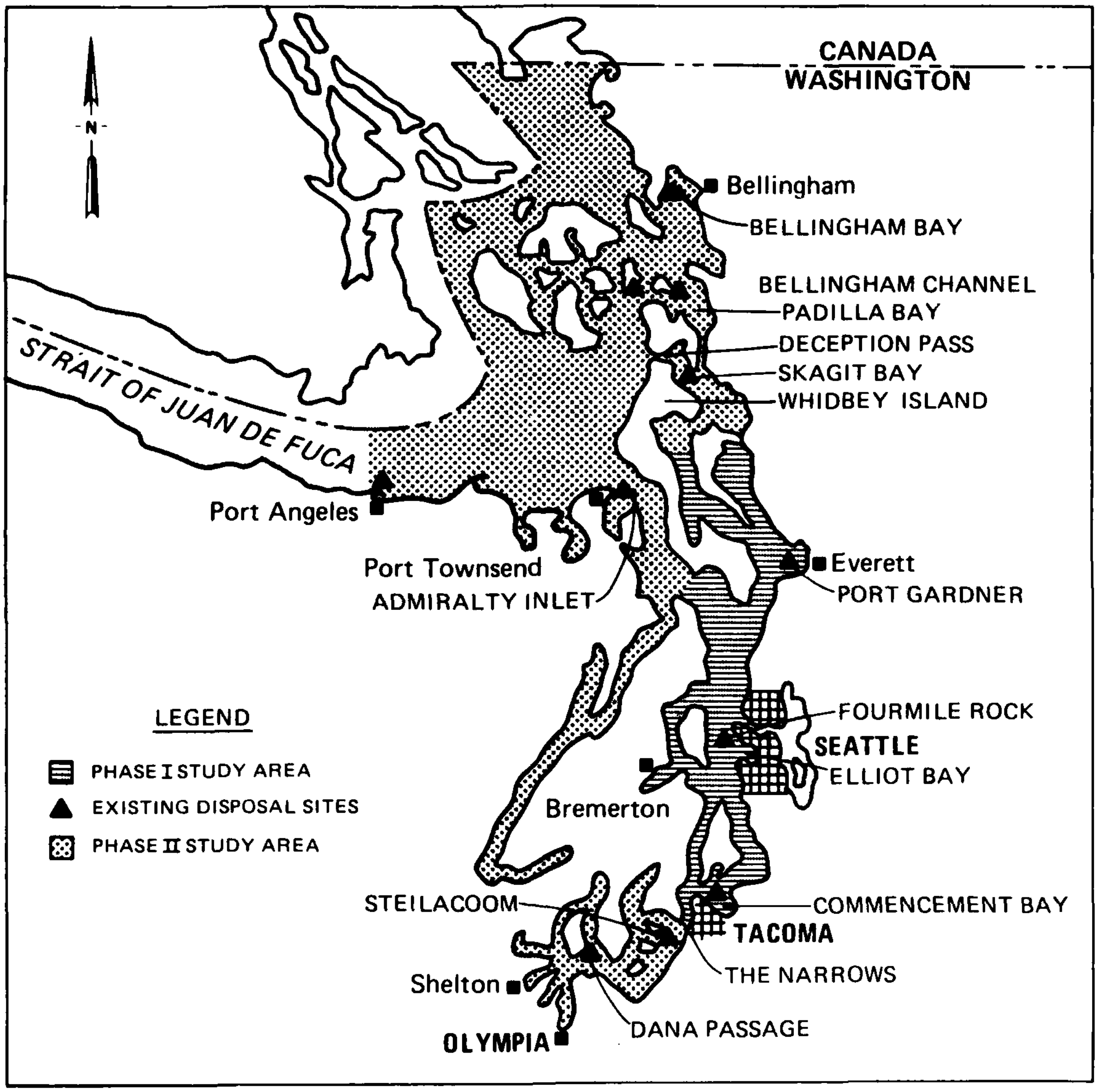

Figure 1. Puget Sound dredge disposal study map

PART II: GENERAL NATURE OF TIDAL CIRCULATION

3. Puget Sound is a fjord-like body of water situated entirely within the State of Washington, as shown in Figure 2 (Crean 1978), but it is

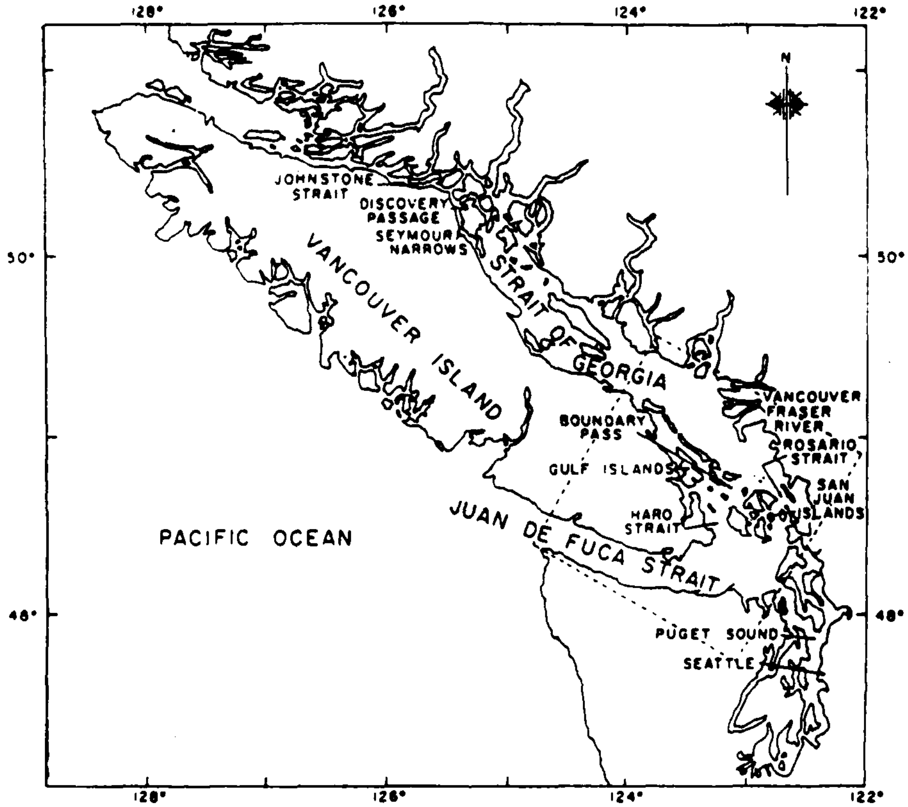

Figure 2. General configuration of the region

contiguous to several major population centers in the United States and Canada. It connects through Admiralty Inlet and Deception Pass to the Strait of Juan de Fuca on the Pacific Ocean (Figure 1). Approximately 98 percent of the tidal prism flows through Admiralty Inlet over a sill of about 64 m near Port Townsend. The main basin has depths in excess of 200 m; it extends south about 60 km from the major junction with Admiralty Inlet near Possession Point to the Narrows (a constriction of about 44 m sill depth). Within the main basin the 183-m contour delineates a deeper section that is roughly 50 km long and 3 to 5 km wide. Other subdivisions of the system include Hood Canal, the Whidbey Basin, and the Southern Basin. Numerous rivers provide fresh water into the Puget Sound System. But the Skagit, entering from the north, is credited with supplying over 60 percent of the fresh water.

4. Flow in Puget Sound is strongly modified by vertical mixing of surface and deep water over the sills as the water moves between the basins. Parker (1977) has investigated the tidal characteristics in the Strait of Juan de Fuca-Strait of Georgia system. The harmonic analysis results from 95 tide stations and 105 current stations have been used to construct M_2 and K_1 amplitudes and phase diagrams. These tidal constituents are by far the dominant semidiurnal and diurnal components in the local tidal regime. Parker (1977) notes that the major features of the tidal hydrodynamics are:

a. The tidal wave is almost pure standing in the Strait of Georgia and much closer to pure progressive in the Strait of Juan de Fuca.

b. The type of tide is mixed and mainly diurnal.

c. The type of tidal current is everywhere mixed and mainly semidiurnal, although it is close to being semidiurnal in places; K_1/M_2 amplitude ratios for the tidal current are generally much less than for the tide except where certain geographical influences play a role.

d. The basin is wide enough for Coriolis effects to bring about as much as a 0.4-m increase in the M_2 tide range in the area.

Additional studies of tidal characteristics in the approaches to Puget Sound have been performed by Cannon et al. (1978), Holbrook et al. (1980), and Parker and Bruce (1980).

5. Communication between the Strait of Juan de Fuca-Strait of Georgia system occurs primarily through Admiralty Inlet with a weak secondary path through Deception Pass. Both Admiralty Inlet and Deception Pass have entrance sills. The Admiralty Inlet sill structure extends for approximately 31 km and consists of two sills at each end of an interior region over 150 m deep. Cannon and Laird (1980) have investigated the characteristics of flow over the Admiralty Inlet sill during deepwater renewal in the Central Basin. Intrusions of new deep water have been shown by hydraulic model studies to occur when floodtide ranges at Seattle exceed 3.5 m. Under this condition, Strait of Juan de Fuca water transits the Admiralty Inlet sill in one flood period and thus is least mixed with Central Basin water. Deepwater replacement then occurs.

6. However, Cannon and Laird (1980) also report deepwater replacement during low tidal ranges in early spring and fall. Cannon and Laird speculate that the water outside the entrance sill in the Strait of Juan de Fuca is sufficiently dense relative to the water in the main basin interior to the sill

and that even though more than one tidal cycle is required to transit the sill causing further mixing and reduction in density, bottom water renewal still occurs. During the renewal process, a strong downwelling of outward flowing surface water occurs and is refluxed into the landward flowing bottom water. At the opposite end of the main basin, a major region of upwelling is tidally induced by high currents through the Narrows. The flow regime is, therefore, highly three-dimensional in the sill zones interior to the Central Basin.

7. Geyer and Cannon (1982) explore the sill processes related to deep-water renewal in a fjord. Because of the extremely long (over 30 km) entrance sill at Admiralty Inlet, tidal mixing of the overlying water is significantly increased from normal entrance sills on the order of 1 km in length. Water denser than the deep water of Puget Sound is always present above sill depth to seaward of the sill. Vertical mixing generally prohibits the dense water from transmitting the sill zone into the main basin. Bottom water renewal is apparently controlled by changes in the intensity of this mixing because of fortnightly variations in tidal amplitude. The interaction of tidal flow and low-frequency baroclinic circulation in Puget Sound appears to be of first-order significance in the behavior of the baroclinic field.

8. Cannon et al. (1984) have attempted to develop seasonal estimates of transport for the main basin based upon long-term current measurements in the bottom layer off Seattle. They report an average replacement time of less than 2 weeks when bottom renewal is occurring. The reflux phenomena appear to be extremely complex when the effects of Whidbey Basin, Hood Canal, and Southern Basin are taken into account. Cannon et al. (1984) report that there appears to be a delicate balance of forces along the main basin because of relatively small horizontal gradients. In this case, wind contribution to the total horizontal pressure gradient may result in significant flow adjustment throughout the water column.

9. Cannon (1983) has provided an overview of circulation in the Puget Sound estuarine system in which he addresses the significance of the coastal interaction through the Strait of Juan de Fuca. The influence of the fresh-water source from the Fraser River may also be felt in Puget Sound. Coastal storms generate flow reversals with inflow near the surface and outflow near the bottom. The highly complex three-dimensional flow field in the approaches to Puget Sound appears to be influenced by coastal storm systems, seasonal

temperature cycles, seasonal freshwater inflows, and winds and pressure patterns.

10. McGary and Lincoln (1984) present tidal prints which depict tidal circulation at eight tide stages for the major divisions of Puget Sound. General physical characteristics of Puget Sound are given by McGary and Lincoln (1984) in Table 1. Cox et al. (1984a,b,c) synthesize current measurements in a three-volume index. Table 2 summarizes the measurement effort. Volume 1

Table 1

Physical Characteristics of Puget Sound

Characteristic	Value	
Water area at mean high water	767.6	square miles (nautical)*
Length of shoreline	1,157	miles (nautical)
Total volume below mean high water	26.5	cubic miles (nautical)
Mean tidal exchange	1.27	cubic miles (nautical)
Average depth	34	fathoms
Maximum depth (off Point Jefferson)	155	fathoms
Maximum currents, Deception Pass	9-10	knots
The Narrows	5.5	knots
River Discharge		
Maximum monthly average	367,000	cfs
Yearly mean	41,000	cfs
Minimum monthly average	14,000	cfs

* A table of factors for converting non-SI units of measurement to SI (metric) units is presented on page 3.

Table 2

Puget Sound Current Measurements

Location	Years of Data	Sites
Whidbey Basin	5.3	47
Admiralty Inlet	9.2	78
Main Basin	24.5	101
Hood Canal	4.8	31
Southern Basin	10.1	83

details current measurements in Puget Sound from 1908 to 1980. Runoff, air temperature, wind, and sea level records are also presented in Volume 2 for several periods of current measurements in order to determine their influence on circulation patterns. In Volume 3, an interpretation of the circulation in Puget Sound is made based upon an interpretation of historical current records.

11. The variance of oscillating currents in the sill zones of the system exceed those in the main basin by one to two orders of magnitude. The variance ratio over the sills to the basins is less everywhere except in the Narrows and Admiralty Inlet. A moderate change in the sill zones occurs in salinity, dissolved oxygen, and temperature when water transverses the near surface and bottom. Three categories of vertical profiles exist in the system: single-layer flow, two-layer flow, and unresolved flow. Areas of single-layer flow are the western shore of Whidbey Island, Colvos Passage, northern and southern East Passage, Dalco Passage, and Balch Passage. Two-layer flow is generally seen over sills and within the basins. Dabob Bay and Hood Canal are in the category of unresolved flow because their speeds are too slow to reveal a distinct pattern. Compared with the basins, many of the sill zones are quite energetic. The main basin is enclosed by two of the more energetic sill zones, causing it to have a vigorous, rapid circulation year round which is tempered by wind action. Mofjeld and Larsen (1984) have investigated tides and tidal currents of the inland waters of western Washington. They report that the tides in the region are formed by long waves which propagate into the system from the Pacific Ocean and reflect to form patterns of nearly standing waves. The tidal motions of the region are subject to extremely strong dissipation concentrated in channels connecting the major basins or near the heads of the system. Coriolis and nonlinear effects are also important.

12. General tidal characteristics at selected stations are given in Mofjeld and Larsen (1984). Parker (1977) gives the following definitions for the types of tides:

a. Semidiurnal: $K_1 + 0_1/M_2 + S_2 < 1/4$; two tidal cycles per day with usually both high waters and both low waters of approximately equal height.

b. Mixed, mainly semidiurnal: $1/4 < K_1 + 0_1/M_2 + S_2 < 1\text{-}1/2$; usually two tidal cycles per day with inequalities in height

and time of successive high waters and/or low waters. (These inequalities reach their peak when the declination of the moon has passed its maximum.)

c. Mixed, mainly diurnal: $1\text{-}1/2 < K_1 + O_1/M_2 + S_2 < 3$; usually two cycles per day with large inequalities when the moon is over the equator, and one cycle per day when the moon is near maximum declination.

d. Diurnal: $K_1 + O_1/M_2 + S_2 > 3$; usually one cycle per day.

Lunitidal interval is the time elapsed from Greenwich transit until high water of the M_2 tidal constituent. Phase age is the time elapsed from the full or new moon until the maximum semidiurnal tide. Parallax age is the time elapsed from lunar perigee (moon closest to the earth) until the maximum semidiurnal lunar tide. Diurnal age represents the time elapsed from maximum diurnal forcing until maximum diurnal tide.

13. When the tide is mixed, the relative heights of successive high and low water depend on the epochs of M_2 , K_1 , and O_1 . Parker (1977) gives the following four cases:

a. $M_2^\circ - K_1^\circ - O_1^\circ = O_1^\circ$: low waters are equal; the inequality is all in the high waters.

b. $M_2^\circ - K_1^\circ - O_1^\circ = 90^\circ$: the inequality between high waters equals the inequality between low waters; the sequence of the tide is higher high water, lower low water, lower high water, and higher low water.

c. $M_2^\circ - K_1^\circ - O_1^\circ = 180^\circ$: high waters are equal; the inequality is all in the low waters.

d. $M_2^\circ - K_1^\circ - O_1^\circ = 270^\circ$: The inequality between high waters equals the inequality between low waters; the sequence of the tide is lower low water, higher high water, higher low water, and lower high water.

For $M_2^\circ - K_1^\circ - O_1^\circ < 180^\circ$, there are inequalities in both high waters and low waters, with more inequality in the lows, though less so as this value decreases. The sequence of the tide is higher high water, lower low water, lower high water, and higher low water. For $M_2^\circ - K_1^\circ - O_1^\circ > 180^\circ$, the same is true, except the sequence of the tide is lower low water, higher high water, higher low water, and lower high water.

14. Tides are mixed-semidiurnal in Puget Sound. At the entrances to Admiralty Inlet and Deception Pass the tides are mixed diurnal because of the cancellation of incident and reflected semidiurnal waves. The phase

relationships produce nearly equal high waters with large differences in the low waters when the moon is away from the equator. Near the winter and summer solstices, when the sun is at maximum declination, large tidal ranges and inequalities coincide. Near spring and fall equinoxes the larger ranges have small inequalities, while the small ranges have large inequalities. In winter the lowest tides occur at night, while during the summer lowest tides are during the day.

15. Mofjeld and Larsen (1984) characterize tidal currents based upon the amplitude of the major axis of the current ellipses. The tidal currents are mixed-semidiurnal in nature. An investigation of the vertical structure of the M_2 and K_1 current components is presented in Figure 3 (Mofjeld and Larsen 1984). Depicted in the figure are vertical profiles of the M_2 (solid circles) and K_1 (solid triangles) tidal currents at selected stations in Admiralty Inlet and the Main Basin of Puget Sound (asterisks indicate equal values for M_2 and K_1). Shown are the amplitudes, Greenwich phase lags, and flood (toward the Southern Basin) direction. Values are from 29-day harmonic analyses of observations by Cannon et al. (1979). There appears to be a uniform depth relationship for the major amplitude and flood direction of the constituent current ellipses, except in the sill zones at Admiralty Inlet and in the Narrows. In Admiralty Inlet there are major diurnal inequalities in both flood and ebb currents; whereas in the Narrows major diurnal inequalities occur in the flood currents only. Tidal prism information given in Table 3 (Mofjeld and Larsen 1984) indicates 24 percent of the M_2 tidal transport entering the eastern Strait of Juan de Fuca is compensated by transport into Puget Sound.

16. Numerous tidal eddies form behind promontories. The movement of these tidal eddies is extremely complex and may interact with tidal fronts. Tidal fronts are the surface expression of convergence zones in which near surface water flows downward at much higher speeds than the magnitude of the vertical velocities caused by the astronomic tide. In Puget Sound strong tidal fronts occur at the ends of Admiralty Inlet and off Foulweather Bluff within the inlet. Tidal currents also generate two types of internal waves. The first type consists of groups of high-frequency internal waves which form over the sills in the vicinity of Colvos Passage. Semidiurnal seiches with vertical excursions as large as 50 m in the depth of the pynocline observed in the Strait of Juan de Fuca comprise the second type.

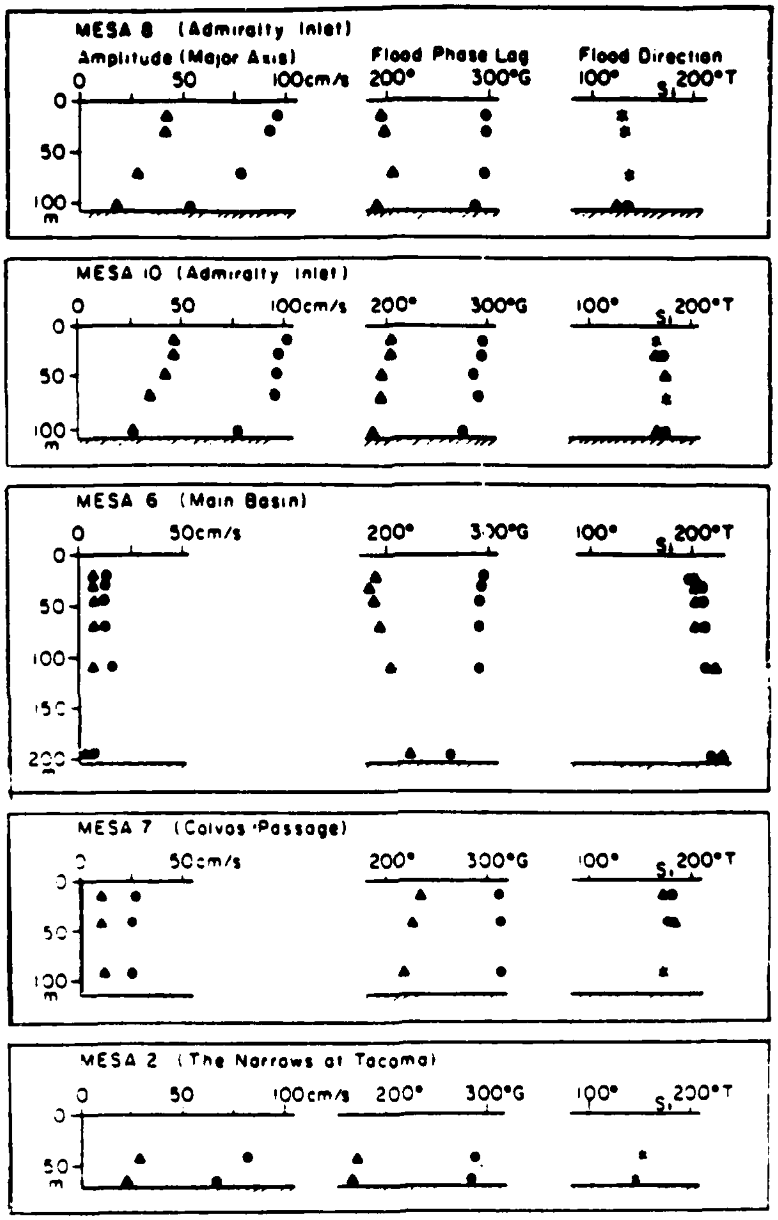

Figure 3. Vertical current structure

Table 3

Puget Sound Tidal Prism by Basin

Basin	Total Volume* km^3	Tidal Prism** km^3	Percentage
Admiralty Inlet	21.7	1.00	4.6
Main Basin	77.0	2.44	3.2
Southern Basin	15.9	1.69	10.6
Hood Canal	25.0	1.14	4.6
Whidbey Basin	29.1	1.83	6.3
Puget Sound	168.7	8.08	4.8

* Volume below mean high water.

** Tidal prism (volume between mean high water and mean lower low water) of Puget Sound.

17. In summary, as Mofjeld and Larsen (1984) note, the general distribution of tides and currents appears to be well established; but the detailed circulation features remain to be resolved. As an initial investigation a two-dimensional modeling approach is undertaken in this study since the disposal site locations are not within the highly energetic sill zones and the vertical flow structure is uniform. Model results in these sill zones should be interpreted with caution.

PART III: TIDE PREDICTION PROGRAM

18. A general tide elevation program was developed following the approach of Shureman (1941). Consider the tidal height $y(t)$ to be given as follows:

$$y(t) = A \cos(at - \zeta) = A \cos[\theta(t)], \text{ with } \theta(t) = (at - \zeta) \tag{1}$$

where

$y(t)$ = height of the tide above some datum as a function of time t

A = tidal amplitude, usually associated with a given constituent

a = tidal speed, usually associated with a given constituent

ζ = phase angle, usually associated with a given constituent

Thus at $t = \zeta/a$, $\theta(\zeta/a) = 0$, and $y(\zeta/a) = A$, $y(t)$ is a maximum (high water). To predict the tide, the following relationship may be used referenced to the local meridian:

$$h(t) = H_o + \Sigma\, fH \cos \overbrace{\left[at_{local} + (V_o + u)_{local} - K\right]}^{\theta(t)} \tag{2}$$

where

$h(t)$ = tidal height at time t

H_o = mean height of the water level relative to the datum

f = factor for reducing mean amplitude to the year of prediction

H = mean amplitude of constituent A

a = solar speed (°/hr) of constituent A

t_{local} = time reckoned from some initial epoch such as the beginning of the year of predictions relative to the local meridian

$(V_o + u)_{local}$ = value of equilibrium argument at the given location where prediction is being made for constituent A at $t_{local} = 0$

K = local epoch of constituent A

19. At $t = 0$: $\theta(0) = (V_o + u)_{local} - K = -\zeta$ and $K = (V_o + u)_{local} + \zeta$. Note the following relation:

$$(V_o + u)_{local} = \text{Greenwich } (V_o + u) - pL + \frac{aS}{15} \tag{3}$$

where

p = constituent subscript

L = local longitude

a = constituent speed (°/solar hour)

S = time meridian (longitude)

If all variables are related to Greenwich, a second prediction formula is given:

$$h(t) = H_o + \Sigma\, fH \cos \overbrace{[at + \text{Greenwich } (V_o + u) - K']}^{\theta(t)} \tag{4}$$

where

$$K' = \text{Greenwich } (V_o + u) - pL + \frac{aS}{15} + \zeta \tag{5}$$

At $t = 0$, $\theta(0) = \text{Greenwich } (V_o + u) - K' = -\zeta$. Rearranging terms and utilizing previous results, one may obtain the following relationships:

$$K' = \zeta + \text{Greenwich } (V_o + u) = \overbrace{\zeta + (V_o + u)_{local}}^{K} + pL - \frac{aS}{15} \tag{6a}$$

$$g = K' = K + ph - \frac{aS}{15} \tag{6b}$$

20. Consider a third prediction equation of the following form:

$$h(t) = H_o + \Sigma\, fH \cos \overbrace{at + \text{Greenwich } (V_o + u) + \frac{aS}{15} - G}^{\theta(t)} \tag{7}$$

where all quantities are as previously defined. At $t = 0$, $\theta(0) = \text{Greenwich } (V_o + u) + aS/15 - G - \zeta$. Therefore, we obtain the following relations:

$$G = \text{Greenwich } (V_o + u) + \frac{aS}{15} + \zeta \tag{8a}$$

$$G = K + pL - aS - \zeta + \frac{aS}{15} + \zeta \tag{8b}$$

$$G = K + pL \tag{8c}$$

Considering Equations 6b and 8c we obtain

$$K' = g = G - \frac{aS}{15} \tag{9}$$

Tidal Elevation Determination

21. The tide program developed considers Equation 5. The start of the prediction period is considered initially in Greenwich mean time (Gmt), and the following set of astronomic arguments is computed based upon relations from Shureman (1941):

T = solar hour angle (degrees)

h = mean longitude of the sun (degrees)

P_1 = longitude of solar perigee (degrees)

S = mean longitude of the moon (degrees)

P = longitude of lunar perigee (degrees)

N = longitude of lunar node (degrees)

22. For tidal elevation, constituent epoch data were obtained in terms of Greenwich phase G from Mofjeld and Larsen (1984) and from the National Ocean Survey (NOS)/National Oceanic and Atmospheric Administration (NOAA)* in terms of the local time meridian g. Equation 9 was used to convert G to g for use in Equation 5.

23. Greenwich $(V_o + u)$ and f were calculated in the program using the above set of astronomic arguments for 1 January 1986 hour zero and 2 July 1986 hour twelve, corresponding to the beginning and middle of 1986. Node factors at the middle of the year were compared with values in Table 14 of Shureman (1941). The equilibrium argument, Greenwich $(V_o + u)$, reported in Table 15 of Shureman (1941) is constructed adding V_o on 1 January zero hour

* Correspondence (dated 27 September 1985) from Elmo E. Long, Oceanographer, Tide and Current Prediction Section, NOS/NOAA, Rockville, Md. (tidal elevation constants for Seattle and Port Townsend and tidal current harmonic constants for Admiralty Inlet).

Gmt to the u referred to the middle of the same calendar year. The equilibrium arguments were constructed from the two initial prediction times and were compared with values in Table 15 of Shureman (1941).

24. Astronomic arguments corresponding to 1 January 1986 hour zero as computed by the program are given in Table 4. Computed values for node

Table 4

Computed Astronomic Arguments, 1 January 1986, Hour Zero Gmt

Symbol	Description	Value, °
N	Longitude of lunar node	35.82160
h	Mean longitude of sun	280.35817
P_1	Longitude of solar perigee	282.69966
S	Mean longitude of lunar perigee	160.82641
P	Longitude of lunar perigee	233.68806
I	Intersection of lunar orbit and equator	27.77788
ξ	Longitude in the lunar orbit	5.83583
γ	Longitude in the celestial equator	6.46613
r'	V prime	4.60062
zr"	V double prime	9.69945
T	Solar hour angle	180.00000

factors and equilibrium arguments are compared versus values given in Shureman (1941) in Table 5. Based upon harmonic constants supplied by NOS (see paragraph 22), for Port Townsend and Seattle, Washington, respectively, the program was used to predict the tide at half-hour intervals for the period 18-22 December 1986. As noted, 30 constituents were considered at Port Townsend, while 25 constituents were used at Seattle. Predicted tidal histories are presented in Plates 1 and 2 for Port Townsend and Seattle, respectively. Based upon the harmonic constants supplied by NOS, tide elevations were predicted at half-hour intervals for the same period as above. For Deception Pass, Victoria, values were used except for the K_1 and M_2 constituents. Amplitudes of 74 and 58 cm, and Greenwich phases of 269 and 345 deg were substituted for the K_1 and M_2 value constituents, respectively.

Table 5

Computed Node Factor and Equilibrium Argument Comparisons

Constituent	Node Factor	Equilibrium Argument (V + U)
M2	0.967	60.0
S2	1.000	0.00
N2	0.967	323.38
K1	1.104	2.36
M4	0.935	120.0
O1	1.168	60.8
M6	0.904	179.99
MK3	1.068	62.36
S4	1.000	0.00
MN4	0.935	23.37
V2	0.967	218.57
S6	1.000	0.00
U2	0.967	121.94
2N2	0.967	226.75
OO1	1.702 (1.706)**	117.59
LB2	0.967	81.44
S1	1.000	180.00
M1	1.291 (1.292)	291.57
J1	1.153	95.81
MM	0.884	96.63
SSA	1.000	199.70
SA	1.000	279.85
MSF*	0.884	298.06 (300.00)†
MF	1.411 (1.412)	118.39
RHO1	1.168	219.37
Q1	1.168	324.17
T2	1.000	2.82
R2	1.000	177.18
2Q1	1.168	227.54
P1	1.000	350.15
2SM2*	0.967	300.00
M3	0.951	270.00
L2	1.266 (1.263)	350.37 (350.3)
2MK3	1.032	117.63
K2	1.285	184.18
M8	0.874	239.99
MS4	0.935	60.0

* Node factors were computed using formulas given in Shureman (1941). In Table 14 (Shureman 1941) the node factor is assumed equal to that of M_2.

** Values in Table 14 (Shureman 1941) if different from computed values.

† Values in Table 15 (Shureman 1941) if different from computed values.

25. Predicted values were calculated using 12, 12, 10, and 8 constituents for Port Townsend, Seattle, Olympia, and Deception Pass, respectively. A comparison of the predicted tide at Port Townsend based on the 12 major constituents (Plate 3) with that based on 30 constituents (Plate 1) reveals the nature of the curves to be very similar. Minor differences in the shapes of the curves are observed in the regions between higher low water and lower high water. Similar features are noted in the comparison of the predicted tide at Seattle based upon the 12 major constituents with that based on 25 constituents. The predicted times and values of high and low waters for this period were compared with values given in the 1986 Tide Tables (US Department of Commerce 1986). Times and values are in good agreement.

Tidal Current Analysis

26. In considering tidal currents, a separate harmonic analysis is performed for each horizontal current component. The horizontal current motion is sensed at several depths, usually in one mooring system. The equations previously developed hold for each horizontal component. As a formal means of determining predominant ebb and flow directions, a current constituent ellipse may be constructed from a knowledge of tidal current component amplitudes and phases. The major axis of the ellipse may then be used to define the predominant ebb-flood directions for each constituent. Usually the orientation of the major axis is very nearly the same for all constituents. Once the predominant ebb-flood direction has been determined, the horizontal velocity component in the flood direction is determined, and a harmonic analysis is performed. One such flood-ebb harmonic analysis was performed at Admiralty Inlet off Bush Point, and the results were reported by NOS/NOAA (see paragraph 22). The program was employed to predict currents along the flood-ebb direction at half-hour intervals for the period 23-27 August 1984. Predicted values in knots (based on a table from the results cited in paragraph 22), are shown in Plate 4 (e.g. the short-period components were not increased by 10 percent). Note that Plate 4 values are plotted about a mean of -0.5 knots. Times of ebb (-peaks) and flood (+ peaks) at Admiralty Inlet shown in Plate 4 compare well with values given in the 1984 Tidal Current Tables (US Department of Commerce 1984).

27. Additional tidal current harmonic constants were furnished by the Pacific Marine Environmental Laboratory* in conjunction with this study. These harmonic constant data were used to predict tidal currents at half-hour increments for Admiralty Inlet, Bush Point, and the northern end of the Narrows. In general, times of ebb and flood predicted by the program are in good agreement with the published values in the 1984 Tidal Current Tables (US Department of Commerce 1984).

28. Data from the tide program are used directly by the numerical hydrodynamic model, both as data for forcing model open boundaries and as input for comparing model results with reconstructed elevation and current hydrographs at interior model locations.

---

* Correspondence (dated 2 August 1985) from Harold O. Mofjeld, Oceanographer, Pacific Marine Environmental Laboratory, Seattle, Wash. (tidal station current ellipses together with charts showing station locations).

PART IV: NUMERICAL LONG-WAVE INVESTIGATION

29. Prior to undertaking a numerical investigation of astronomic tidal circulation in Puget Sound, a brief review of previous modeling efforts was conducted. General circulation characteristics have been studied using a physical model of Puget Sound at the University of Washington. As reported by McGary and Lincoln (1984), the model cannot resolve detailed flow structure through several of the narrow passes (Deception Pass, Hammersley Inlet, Agate Passage) because of surface tension effects associated with the resolution scale. The physical model results, however, may be used as a check on results obtained from numerical models.

30. Water Resources Engineers, Inc. (1985), developed a comprehensive set of mathematical models to simulate the characteristics of the Puget Sound ecosystem. A link-node model developed by Shubinski, McCarty, and Lindorf (1965) and a two-dimensional fjord hydrodynamic model developed by Winter (1973) were utilized to describe the hydrodynamics. A water quality link-node model as reported by Genet, Smith, and Sonnen (1974) was utilized in conjunction with the link-node ecologic package reported by Chen and Orlob (1972). A finite-element approach was also considered as reported by King, Norton, and Orlob (1973). Although specific planning results were not developed, the study did provide the first complete systematic approach to the ecological description of Puget Sound from a numerical modeling perspective. The three dimensionality of the flow structure was also considered on a preliminary basis.

31. Jamart and Winter (1978) utilized a two-dimensional, vertically integrated finite-element model to simulate flow conditions in a portion of Hood Canal. The specification of appropriate open-water boundary conditions was difficult to obtain. Crean (1978) utilized a two-dimensional, vertically integrated finite-difference model to study tidal characteristics of the combined Strait of Juan de Fuca-Strait of Georgia system. The regional extent of the 2-km square grid is shown in Figure 2. As an alternative to a finite-element approach toward grid resolution flexibility, Sheng and Hirsh (1984) have reported a numerical solution of the shallow-water equations in a boundary fitted coordinate system. Three-dimensional efforts toward description of the highly complex tidal flow regime in Puget Sound are currently being pursued at the University of Washington and at the Japanese National

Research Institute for Pollution and Resources.*

32. In an effort to obtain seasonal estimates of transport variability within Puget Sound, Hamilton, Gunn, and Cannon (in press) have developed a box model. At the Pacific Marine Environmental Laboratory a reflux model has been developed to determine residence times associated with the major basins.* These two modeling efforts are directed at seasonal or yearly time scales.

33. Under the present modeling approach, a two-dimensional, vertically integrated set of equations is considered in an exponentially stretched context developed by Butler (1980). The detailed development of the long-wave equation set is presented by Schmalz (1983). Although a compatible three-dimensional hydrodynamic and sediment transport model has been developed (Sheng 1983), the above two-dimensional vertically integrated approach was undertaken in this study because of economic and time constraints, as detailed below.

Puget Sound Global Grid Development

34. In developing the grid for Puget Sound, two global grid alternatives were considered. In the first alternative spatial resolution ΔS was chosen to be 1,500 ft, which roughly corresponds to the diameter of the existing disposal sites. A grid of this resolution would require approximately 15,000 cells. The maximum water depth in Puget Sound is 150 fathoms (900 ft). With this information the gravity wave speed and the explicit time-steps were calculated to be 170 fps and 8.8 sec, respectively. An implicit time-step of 60 sec was considered which resulted in a Courant number of 6.8. Over 5,700 time-steps would be required for a 4-day simulated period at 1,440 time-steps per day. To perform this number of operations over a 15,000-cell grid would be extremely costly. Therefore, a second grid was developed with a spatial resolution of 3,750 ft. A timesharing program was used to develop a 70 × 103 grid totaling 7,210 cells. The explicit and implicit time-steps increased, while the Courant number decreased to 22.06, 90, and 4.08 sec. Because of a reduction from approximately 15,000 to approximately 7,000 cells, a simulation period of 5 days would require 4,800 time-steps at 960 time-steps

* Correspondence (dated 10 October 1985) from Harold O. Mofjeld, Oceanographer, Pacific Marine Environmental Laboratory, Seattle, Wash.

per day. Most of the grid is shown in Figure 4. The section of grid above Skagit Bay is omitted.

Depth field

35. Digitization of the Puget Sound depth field involved the use of Nautical Chart 18440 (Admiralty Inlet and Puget Sound) and Nautical Chart 18421 (the Strait of Juan de Fuca to the Strait of Georgia). Because of the configuration of Admiralty Inlet and Puget Sound, water depths fluctuate rather abruptly from one extreme to the next. For this reason, depths in many cells had to be averaged to obtain a fairly reasonable representative cell depth.

36. A number of small islands that obstruct water flow are located in the area, so barriers were added to make the boundaries more precise. In some instances, points had to be idealized to represent either land or water that would be crucial in model calculations. Only a small portion of Nautical Chart 18421, consisting of the adjacent area in the southeast section of the chart, was needed.

Barrier and boundary system

37. All barriers were located on cell faces and assigned a land elevation of 10 ft. The barriers are modeled as exposed barriers (i.e., no overtopping will occur at any barrier during the simulations). The cell locations are specified using the coordinate system N,M , with N numbered from left to right and M top to bottom.

Tidal signals

38. The tidal signals along the open-water boundary are specified at Port Townsend, Point Partridge, and Deception Pass located at cells 30,24 , 30,20 , and 37,7 , respectively. Of the 37 possible tidal constituents, 12 were considered initially: M_2 , S_2 , N_2 , K_1 , M_4 , O_1 , M_6 , Ssa , Sa , Q_1 , P_1 , and K_2 , as shown in Table 6. In subsequent simulation work the amplitudes and phases of the two long-period constituents Ssa and Sa were set to zero since meteorological effects were not considered in this study.

Elevation and current gage information

39. The numerical behavior of simulated water surface elevation at the 28 stations shown in Table 7 and the simulated currents are compared with predicted values at the 38 current stations specified in Table 8. Tidal currents are reconstructed based upon the M_2 , N_2 , S_2 , O_1 , K_1 , and P_1 tidal

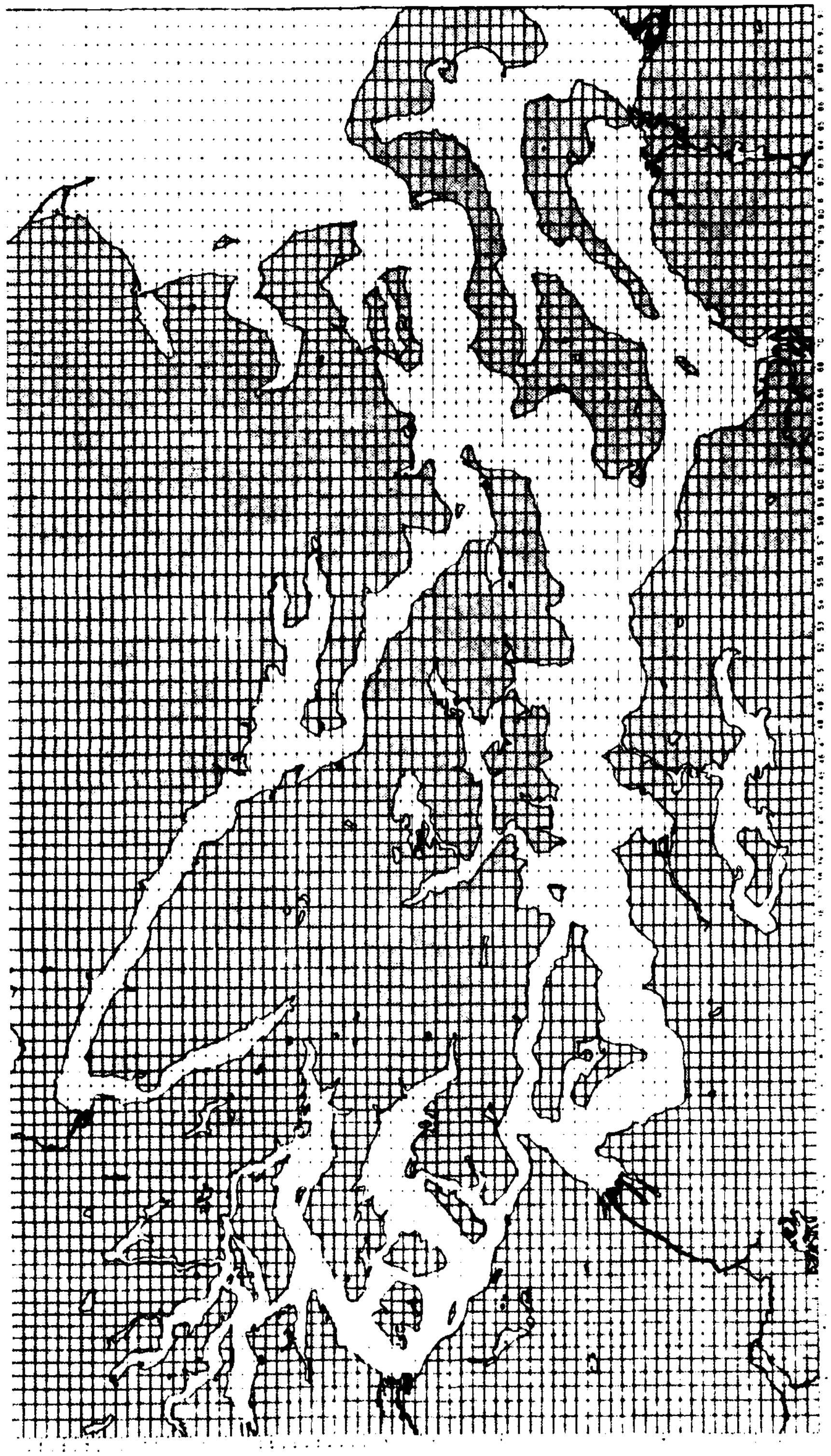

Figure 4. Puget Sound global grid

constituents. However, the tidal elevation boundary signals contain not only these six constituents but also the M_4, M_6, Q_1, and K_2 constituents. This fact should be kept in mind when analyzing subsequent comparisons between simulated and predicted tidal currents. The cells in which disposal sites are located are given in Table 9.

Table 6

Tidal Harmonic Constants for Selected Tide Stations of NOAA

		Port Townsend		Deception Pass*		Point Partridge*	
Tidal Type	Constituent	H, cm	G, °	H, cm	G, °	H, cm	G, °
Long period	Sa	8.0	288	--	--	8.0	288
	Ssa	4.0	225	--	--	4.0	225
Diurnal	Q_1	7.3	242	6.4	239	7.3	242
	O_1	44.3	250	36.3	248	44.3	250
	P_1	24.2	270	19.2	267	24.2	270
	K_1	76.1	271	74.0	269	76.1	271
Semidiurnal	N_2	14.2	321	8.8	286	14.2	321
	M_2	67.0	351	58.0	345	67.0	351
	S_2	16.4	15	10.4	334	16.4	15
	K_2	4.7	18	1.8	341	4.7	18
Quarter diurnal	M_4	4.0	61	--	--	4.0	61
Sixth diurnal	M_6	1.0	249	--	--	1.0	249

* The data for deception Pass are those used for Victoria with changes for K_1 and M_2. The data for Point Partridge are the same as those for Port Townsend.

Table 7

Elevation Gage Locations

Location	Model Indices N,M
Northwest Passage	37,7
Similk Bay	43,5
Skagit Bay	45,12
Lyle Point	35,98
Gig Harbor	43,81
Seattle	58,62
Point Bolin	42,56
Everett	66,38
Admiralty Head	36,24
Port Townsend	31,25
Olympia	21,103
Juan de Fuca	33,19
Freeland	46,35
Livingston Bay	52,20
Hood Head	39,45
Hazel Point	29,56
Dabob Long Spit	27,48
Lynch Cove	22,74
Shelton	9,90
Dyes Inlet	35,59
Bremerton	39,66
Belfry	26,76
Purdy	39,77
Quartermaster Harbor	51,75
Tacoma	52,85
Lower Eld Inlet	14,102
Oyster Bay	11,98
Skookum Inlet	10,96

Table 8

Current Gage Locations

Current Station+	Model Indices N,M	Basin
C-78	31,24	Admiralty Inlet
C-130	40,27	Admiralty Inlet
C-131	37,35	Admiralty Inlet
C-132	39,34	Admiralty Inlet
C-134	32,27	Admiralty Inlet
C-135	39,23	Admiralty Inlet
C-136	39,43	Admiralty Inlet
C-137	41,44	Admiralty Inlet
C-138	43,41	Admiralty Inlet
C-139	43,40	Admiralty Inlet
C-140	44,40	Admiralty Inlet
C-143	50,43	Admiralty Inlet
C-144	58,43	Whidbey
C-145	59,40	Whidbey
C-147	58,36	Whidbey
C-148	58,29	Whidbey
C-149	52,29	Whidbey
C-150	44,22	Whidbey
C-151	54,45	Central
C-152	52,49	Central
C-154	51,55	Central
C-155	46,65	Central
C-156	51,64	Central
C-159	52,69	Central
C-160	54,69	Central
C-161	58,76	Central
C-162	45,54	Central
C-163	47,82	Central
C-164	45,79	Central
C-165	45,83	Central

(Continued)

Table 8 (Concluded)

Current Station+	Model Indices N,M	Basin
C-166	50,58	Central
C-167	54,72	Central
C-176	35,98	Southern
C-177	33,92	Southern
C-178	29,94	Southern
C-179	23,94	Southern
C-180	26,89	Southern
C-181	24,83	Southern

Table 9

Disposal Site Locations

Location	Model Indices N,M
Skagit Bay	11,45
Admiralty Inlet	25,34
Port Gardner	40,64
Fourmile Rock	60,53
Commencement Bay 1	84,50
Commencement Bay 2	85,52
Steilacoom 1	87,41
Steilacoom 2	92,40
Dana Passage	92,25

Calibration Period

40. The period 16-18 January 1981 constituted a spring tide period and was considered as the calibration period. A 90-sec time-step was used in each of 2,880 steps to encompass this 72-hr period. The following paragraphs discuss the bottom friction mechanics which were calibrated.

41. A Manning's n /Chézy C formulation is used to represent bottom friction. Initially, a Manning's n concept is used. The Chézy C is computed as follows:

$$C = \frac{1.49}{n^*} R^{1/6} \tag{10}$$

where

C = Chézy C friction factor

n^* = Manning's n (effective)

R = depth of flow or hydraulic radius

The effective Manning's n is given by the following revised form:

$$n^* = n + (k_1 - n)\left[1 - e^{-0.5\left(d/k_2\right)^3}\right] \tag{11}$$

where

n = Manning's n (specified on input)

k_1 = canopy coefficient 1

d = still-water depth

k_2 = canopy coefficient 2

(Note: $d \to 0 \quad n^* \to n$; $d \to \infty \quad n^* \to k_1$)

42. Thus k_1 corresponds to the deepwater roughness, while n corresponds to the canopy roughness. In the Puget Sound applications, $k_2 = 1$; and $k_1 = n$ where n is specified. The calibrated values of n as a function of still-water depth are as given in Table 10.

43. To improve the comparison between predicted and simulated elevations in the Southern Basin, a special Manning's n of 0.09 is used in The Narrows because of the extremely high rates of dissipation which occur through the interconnecting passages between major basins.

44. Crean (1978), in a study of the Strait of Juan de Fuca-Strait of Georgia System, utilized a dimensionless friction factor $k = 0.03$ in the narrow interconnecting passages in a two-dimensional, depth-averaged transport context. We assume the following correspondence holds with the present velocity formulation:

$$k = \frac{g}{C^2} \qquad (12)$$

where

k = dimensionless friction factor

g = acceleration due to gravity

Table 10

Calibrated Manning's n Friction Factors

Depth Range, ft*	Specified Manning's n
800-900	0.030
700-800	0.031
600-700	0.032
500-600	0.033
400-500	0.034
0-400	0.035

* Mean lower low water (mllw).

45. For $k = 0.03$, $C = 32.76$. In the open strait areas, Crean (1978) used $k = 0.003$ yielding $C = 103.6$. With the Manning's n relation specified in Table 10, the Chézy C under still-water conditions ranges from 75 to 120.5, along a transect opposite Seattle in the Central Basin, to a range from 38 to 42 through The Narrows. The series of calibration simulations and their resulting characteristics is presented in Table 11. Results for Simulation No. 3, representing the final calibration, are depicted in Plates 5-8 for water surface elevations. In these plates the suffix .B. denotes a specified boundary, .S. denotes simulated, and .P. denotes predicted. In Plates 5 and 6, the specified boundary values for the simulation exactly match the predicted values. This matching ensures that the boundary value problem associated with this period is properly specified.

46. In Plates 7 and 8, simulated values are compared with predicted values at Seattle in the Central Basin and at Olympia in the Southern Basin. While simulated results at Seattle show close agreement with predicted values in amplitude and phase, at Olympia the simulated phase and predicted phase show some discrepancy (2 to 3 hr difference). At Olympia, simulated ranges from lower low water to the next high water also show some discrepancy from

predicted behavior. The representation of The Narrows appears to be extremely crucial in the simulation results.

Table 11

Calibration Simulation Series

Simulation No.	Description	Result
1	No special friction treatment in The Narrows	Extreme overprediction of tidal elevations in the Southern Basin
2	Special treatment of friction in The Narrows (0.04-0.05)	Same results as in No. 1
3	Special treatment of friction in The Narrows (0.09)	Improved results in Southern Basin
4	Increased the width of The Narrows (One flow path used standard friction while the second flow path used special (0.09) friction.)	Results similar to those in No. 1
5	Returned to original width of The Narrows (increased friction (0.09) for the Northernmost three cells)	Results similar to those in No. 1

47. Simulated, vertically-averaged currents for the 16-18 January 1981 calibration period based upon the 10 short-period constituents shown in Table 6 were compared with predicted values reconstructed from the three largest semidiurnal constituents M_2, N_2, and S_2 and diurnal constituents O_1, K_1, and P_1, respectively, in the four major basins. In the Admiralty Inlet Basin simulated, vertically-averaged currents are in reasonable agreement with predicted values at various depths. Since the Admiralty Inlet Basin contains a large region of shear flow, some discrepancies are to be expected. In the Whidbey Basin, which is less energetic, simulated, vertically-averaged currents are in excellent agreement with predicted values. In the Central Basin simulated, vertically-averaged currents are in good agreement with predicted values except for station C-162 at the northern entrance of Agate Passage. Because of the limits of resolution in the grid, flow effects associated with this passage could not be simulated. As a result, it is anticipated that local flow effects at station C-162 account for the underestimation of correct magnitude of the simulation results. Simulated, vertically-averaged currents are in general agreement with predicted results in the

Southern Basin. Some discrepancies in current directions are noted at stations C-176 and C-177.

48. Simulated, vertically-averaged currents were examined for each cell in which an existing disposal site is located. Cell-centered velocities, because of the limits of resolution in the grid, do not represent the best estimate of velocity conditions at the site, except at Admiralty Inlet (Plate 9). In order to estimate disposal site velocity characteristics, cell velocity components at the bottom and right cell faces were used directly. The maximum current speed so obtained is presented in Table 12 for the last 2 days (17-18 January 1981) of the 3-day simulation period. At Admiralty Inlet, a range of maximum speed values is presented. The upper value of the range corresponds to the cell-centered maximum velocity magnitude shown in Plate 9.

Table 12

Disposal Site Current Extremal Analysis for the 17-18 January 1981 Spring Tide Period

Disposal Site	Grid Indices N,M	Maximum Current, fps
Skagit Bay	45,11	5.9
Admiralty Inlet	34,25	6.3 - 7*
Port Gardner	64,40**	0.1
Fourmile Rock	53,60	0.5
Commencement Bay 1	50,84	0.4
Commencement Bay 2	52,85	0.1
Steilacoom 1	41,87	1.0
Steilacoom 2	40,92	1.9
Dana Passage	25,92	2.1

* Used cell-centered estimate.
** Used face of cell 64,39 for velocity magnitude.

Verification Period

49. The period 13-15 January 1981 constituted a neap tide period and was utilized as a verification period. As in the calibration period,

2,880 time-steps, each of 90-sec duration, were used to simulate the 72-hr period. The calibrated bottom friction relations shown in Table 10 were used without modification. In general, the simulated water surface elevations for the 13-15 January period are in good agreement with predicted levels. As noted in the 17-18 January calibration, the simulated water surface elevation at Olympia again appears to lag behind the predicted level by 2-3 hrs, and the simulated range in elevation exceeds the predicted range of water levels.

50. Simulated, vertically-averaged currents, for the 13-15 January verification, were generated by specifying the 10 short-period constituents of Table 6 at the respective boundaries. These values were compared with predicted values for the four major basins. Again, the simulated, vertically-averaged currents were found to be in reasonable agreement with predicted values at various depths under the proviso discussed in the calibration section.

51. The best estimate of maximum current at existing disposal sites is presented in Table 13 for the last days of the 3-day simulation period. In

Table 13

Disposal Site Current Extremal Analysis for the 13-15 January 1981 Neap Tide Period

Disposal Site	Grid Indices N,M	Maximum Current, fps
Skagit Bay	45,11	5.0
Admiralty Inlet	34,25	5.5 - 6.1*
Port Gardner	64,40**	0.04
Fourmile Rock	53,60	0.5
Commencement Bay 1	50,84	0.3
Commencement Bay 2	52,85	0.05
Steilacoom 1	41,87	1.0
Steilacoom 2	40,92	1.8
Dana Passage	25,92	1.7

* Cell-centered velocity magnitude.
** Used face of cell 64,39 for velocity magnitude.

general, current speeds are slightly lower during this period than they were during the spring tide calibration period, although regions of high current speeds are noted again in Admiralty Inlet, Deception Pass, and through The Narrows.

Extreme Spring Tide Simulation Period

52. To investigate current magnitudes under extreme astronomic tide conditions, the period 11-13 December 1985 was considered. This period was also selected to coincide with the tidal current measuring program that was conducted by NPS. Maximum vertically-integrated current magnitudes and their times of occurrence are presented in Table 14 at the existing and at PSDDA proposed disposal sites. Simulated water surface elevations are compared with predicted values in Plates 10-12. (Note the 12-ft and almost 11-ft predicted tidal ranges at Port Townsend and Deception Pass, respectively.) The simulated tidal elevations correspond to predicted levels at Seattle in Plate 12 reasonably well, even at this extreme tidal range. Simulated cell-centered velocity histories are shown in Plates 13-17 for the cells in which existing disposal sites are located.

Table 14

Disposal Site Current Extremal Analysis for the

11-13 December 1985 Spring Tide Period

Existing Disposal Site	Grid Indices N,M	Time of Maximum Current*	Maximum Current fps
Skagit Bay	45,11	56.2	6.3
Admiralty Inlet	34,25	50.4	7.0 - 7.9**
Port Gardner	64,40†	50.7	0.1
Fourmile Rock	53,60	69.8	0.6
Commencement Bay 1	50,84	53.5	0.4
Commencement Bay 2	52,85	51.8	0.1
Steilacoom 1	41,87	35.0	1.0
Steilacoom 2	40,92	54.5	2.1
Dana Passage	25,92	53.2	2.4
Proposed PSDDA Site			
Elliott Bay	56,62	70.7	0.1
Port Gardner Bay	62,38	50.8	0.3
Commencement Bay	50,83	53.8	0.4

* Time, in hours, measured from 11 December 1985 hour zero.
** Used cell-centered velocity magnitude.
† Used cell 64,39 velocity magnitude and corresponding time.

PART V: SUMMARY AND CONCLUSIONS

53. Flow in fjord-like Puget Sound is strongly modified by intense vertical mixing of surface and deep water over the sills. Entrance and exit sill zones are associated with Admiralty Inlet, while single sill zones occur at Deception Pass, the Narrows, and the entrances to Hood Canal and Dabob Bay.

54. Tidal elevations are classified as mixed-semidiurnal except at the northern and eastern entrances to Admiralty Inlet and Deception Pass, respectively, where they are mixed-diurnal. Tidal currents are mixed-semidiurnal throughout Puget Sound. Upon the tidal circulation, a time varying gravitational circulation must also be superimposed. Daily average currents illustrate a two-layer system with seaward flow in the top layer and inward-directed bottom layer flow. A reflux, or downwelling, of the seaward surface flow is associated with tidally-induced renewals of bottom water at the southern sill at Admiralty Inlet. These episodes of bottom water renewal appear to occur at irregularly spaced forthnightly intervals.

55. Tidal currents appear to be vertically homogeneous, except in the vicinity of freshwater inflow and in the intense regions of mixing and shear occurring in portions of the sill zones and their entrances.

56. A general tide prediction program based upon Shureman (1941) has been developed to predict tidal elevations and current components. The program was verified by comparing predicted tidal elevations at Port Townsend and Seattle for 18-22 December 1986 with heights of high and low water and times of occurrence published in the 1986 Tide Tables (US Department of Commerce 1986). As an additional check, ebb and flood currents were predicted and compared with values published in the 1984 Tide Current Table (US Department of Commerce 1984) for the period 23-27 August 1984.

57. Astronomic tidal characteristics have been studied on a single global grid encompassing Puget Sound using the two-dimensional, vertically-integrated hydrodynamic WES Implicit Flooding Model (WIFM). The grid dimension of 70 (horizontal) by 103 (vertical) represents 7,210 cells with a maximum spatial resolution of 3,750 feet. A 90-sec time-step was employed in all WIFM long-wave computations resulting in a maximum Courant number of 4.1.

58. Simulated tidal elevations and vertically-averaged currents were calibrated to predicted levels and currents at stations shown in Table 8. Calibrated values of bottom friction are given in Table 10. In order to

reduce simulated tidal amplitudes in the Southern Basin, it was necessary to use a Manning's n of 0.09 through the Narrows. This high friction value is consistent with values used by Crean (1978) in a study of the Strait of Juan de Fuca-Strait of Georgia system. Simulated tidal amplitudes and currents for the 16-18 January 1981 calibration period were generally in good agreement with predicted values except for some discrepancies in the Southern Basin. Peak currents at disposal sites for the 17-18 January 1981 period are shown in Table 12.

59. Bottom friction mechanics previously calibrated to the 16-18 January 1981 spring tide period were verified using the 13-15 January 1981 neap tide period. Simulation results correspond to predicted values of elevation and current except for previously mentioned discrepancies in the Southern Basin. Peak currents at existing disposal sites for the 13-15 January period are shown in Table 13.

60. The 11-13 December 1985 extreme spring tide period was also simulated. Extreme tidal ranges of 12 and 11 ft were used for the Port Townsend and Deception Pass boundary conditions, respectively. Maximum current magnitudes and their associated times of occurrence are given in Table 14.

61. The following conclusions are drawn based upon the results of this investigation. A 7,210-cell global grid encompassing the entire Puget Sound has been developed. Computed tidal elevations and currents are in good agreement with values predicted using harmonic constants. Some discrepancies, particularly in tidal elevations, are noted in the Southern Basin, which is outside the Phase I PSDDA program study area. However, model current results may be used in the Southern Basin as preliminary estimates of vertically-averaged conditions for disposal site management planning purposes. Within the available resolution, model results may be used as reliable estimates of vertically-averaged current conditions at the disposal sites in the Admiralty Inlet, Whidbey, and Central basins. Results are not applicable where large-scale vertical shear takes place, such as at the entrance sills or in the vicinity of large freshwater inflows.

REFERENCES

Butler, H. L. 1980. "Evolution of a Numerical Model for Simulating Long-Period Wave Behavior in Ocean-Estuarine Systems," in Estuarine and Wetland Processes, Hamilton, P. and MacDonald, K., eds., Plenum Press, New York.

Cannon, G. A. 1983 (Jun). "An Overview of Circulation in the Puget Sound Estuarine System," National Oceanic and Atmospheric Administration Technical Memorandum ERL PMEL-48, Pacific Marine Environmental Laboratory, Seattle, Wash.

Cannon, G. A., and Laird, N. P. 1980. "Characteristics of Flow Over a Sill During Deep Water Renewal," in Fjord Oceangraphy, Freeland, H. J. et al., eds., Plenum Press, New York.

Cannon, G. A. et al. 1978 (Jun). "Circulation in the Strait of Juan de Fuca: Some Recent Oceanographic Observations," National Oceanic and Atmospheric Administration Technical Report ERL 399-PMEL 29, Rockville, Md.

__________. 1979. "Puget Sound Circulation: Final Report for FY 77-78," National Oceanic and Atmospheric Administration Technical Memorandum, ERL MESA-40, Rockville, Md.

__________. 1984. "Transport Variability in a Fjord," Contribution No. 681, Pacific Marine Environmental Laboratory, National Oceanic and Atmospheric Administration, Seattle, Wash.

Chen, C. W., and Orlob, G. T. 1972. "Ecologic Simulation for Aquatic Environments," Final Report, prepared for Office of Water Resources Research, Water Resources Engineers, Walnut Creek, Calif.

Cox, J. M. et al. 1984a (May). "Synthesis of Current Measurements in Puget Sound, Washington--Volume 1: Index to Current Measurements Made in Puget Sound from 1908-1980, with Daily and Record Averages for Selected Measurements," National Oceanic and Atmospheric Administration Technical Memorandum NOS OMS-3, Rockville, Md.

__________. 1984b (May). "Synthesis of Current Measurements in Puget Sound, Washington--Volume 2: Indices of Mass and Energy Inputs into Puget Sound: Runoff, Air Temperature, Wind, and Sea Level," National Oceanic and Atmospheric Administration Technical Memorandum NOS OMS-4, Rockville, Md.

__________. 1984c (May). "Synthesis of Current Measurements in Puget Sound, Washington--Volume 3: Circulation in Puget Sound: Interpretation Based on Historical Records of Currents," National Oceanic and Atmospheric Administration Technical Memorandum NOS OMS-5, Rockville, Md.

Crean, P. B. 1978. "A Numerical Model of Barotropic Mixed Tides Between Vancouver Island and the Mainland and its Relation to Studies of the Estuarine Circulation," in Nihoul, J.C.J., ed., Hydrodynamics of Estuaries and Fjords, Elsevier, Amsterdam.

Genet, L. A., Smith, D. J., and Sonnen, M. B. 1974 (May). "Computer Program Documentation for the Dynamic Estuary Model," Intermediate Technical Report, prepared for the US Environmental Protection Agency, Water Resources Engineers, Walnut Creek, Calif.

Geyer, W. R., and Cannon, G. A. 1982 (Sep). "Sill Processes Related to Deep Water Renewal in a Fjord," Journal of Geophysical Research, Vol 87, No. C10, pp 7985-7996.

Hamilton, P., Gunn, J. T., and Cannon, G. L. In press. "A Box Model of Puget Sound, Estuarine, Coastal and Shelf Science."

Holbrook, J. R. et al. 1980 (Apr). "Circulation in the Strait of Juan de Fuca: Recent Oceanographic Observations in the Eastern Basin," National Oceanic and Atmospheric Administration Technical Report ERL 412-PMEL 33, Rockville, Md.

Jamart, B. M., and Winter, D. F. 1978. "A New Approach to the Computation of Tidal Motions in Estuaries," in Nihoul, J.C.J., ed., Hydrodynamics of Estuaries and Fjords, Elsevier, Amsterdam.

King, I. P., Norton, W. R., and Orlob, G. T. 1973 (Apr). "A Finite Element Solution for Two-Dimensional Density Stratified Flow," Final Report to the Office of Water Resources Research, Water Resources Engineers, Walnut Creek, Calif.

McGary, N., and Lincoln, J. H. 1984. Tidal Prints, University of Washington Press, Seattle.

Mofjeld, H. O., and Larsen, L. H. 1984 (Jun). "Tides and Tidal Currents of the Inland Waters of Western Washington," National Oceanic and Atmospheric Administration Technical Memorandum ERL PMEL-56, Pacific Marine Environmental Laboratory, Seattle, Wash.

Parker, Bruce B. 1977 (Jan). "Tidal Hydrodynamics in the Strait of Juan de Fuca-Strait of Georgia," National Oceanic and Atmospheric Administration Technical Report NOS 69, Rockville, Md.

Parker, Bruce B., and Bruce, James T. 1980 (Aug). "Puget Sound Approaches Circulation Survey," National Ocean Service Oceangraphic Circulatory Survey Report No. 3, National Oceanic and Atmospheric Administration, Rockville, Md.

Schmalz, R. A. (1983). "The Development of a Numerical Solution to the Transport Equation; Report 1: Methodology," Miscellaneous Paper CERC-83-2, US Army Engineer Waterways Experiment Station, Vicksburg, Miss.

__________. (1985). "User Guide for WIFM-SAL: A Two-Dimensional Vertically Integrated, Time-Varying Estuarine Transport Model," Instruction Report EL-85-1, US Army Engineer Waterways Experiment Station, Vicksburg, Miss.

Sheng, Y. P. (1983). "Mathematical Modeling of Three-Dimensional Coastal Currents and Sediment Dispersion: Model Development and Application," Technical Report CERC-83-2, US Army Engineer Waterways Experiment Station, Vicksburg, Miss.

Sheng, Y. P., and Hirsh, J. E. 1984 (Apr). "Numerical Solution of Shallow Water Equations in Boundary Fitted Grid," Technical Memorandum 84-15, Aeronautical Research Associates of Princeton, Inc., N.J.

Shubinski, R. P., McCarty, J. C., and Lindorf, M. R. 1965 (May). "Computer Simulation of Estuarial Networks," Journal of the Hydraulics Division, Americal Society of Civil Engineers, Vol 91, No. HY5.

Shureman, Paul. 1941. Manual of Harmonic Analysis and Prediction of Tides, Special Publication 98, US Coast and Geodetic Survey, National Oceanic and Atmospheric Administration, Rockville, Md.

US Department of Commerce. 1984. Current Tables--Pacific Coast of North America and Asia, National Oceanic and Atmospheric Administration, Rockville, Md.

__________. 1986. Tide Tables--High and Low Water Predictions, West Coast of North and South America, National Oceanic and Atmospheric Administration, Rockville, Md.

Water Resources Engineers, Inc. 1985. Ecologic Modeling of Puget Sound and Adjacent Waters, prepared for the Environmental Protection Agency, Walnut Creek, Calif.

Winter, D. F. 1973. A Simulation Solution for Steady-State Gravitational Circulation in Fjords, Department of Oceanography, University of Washington, Pullman, Wash.

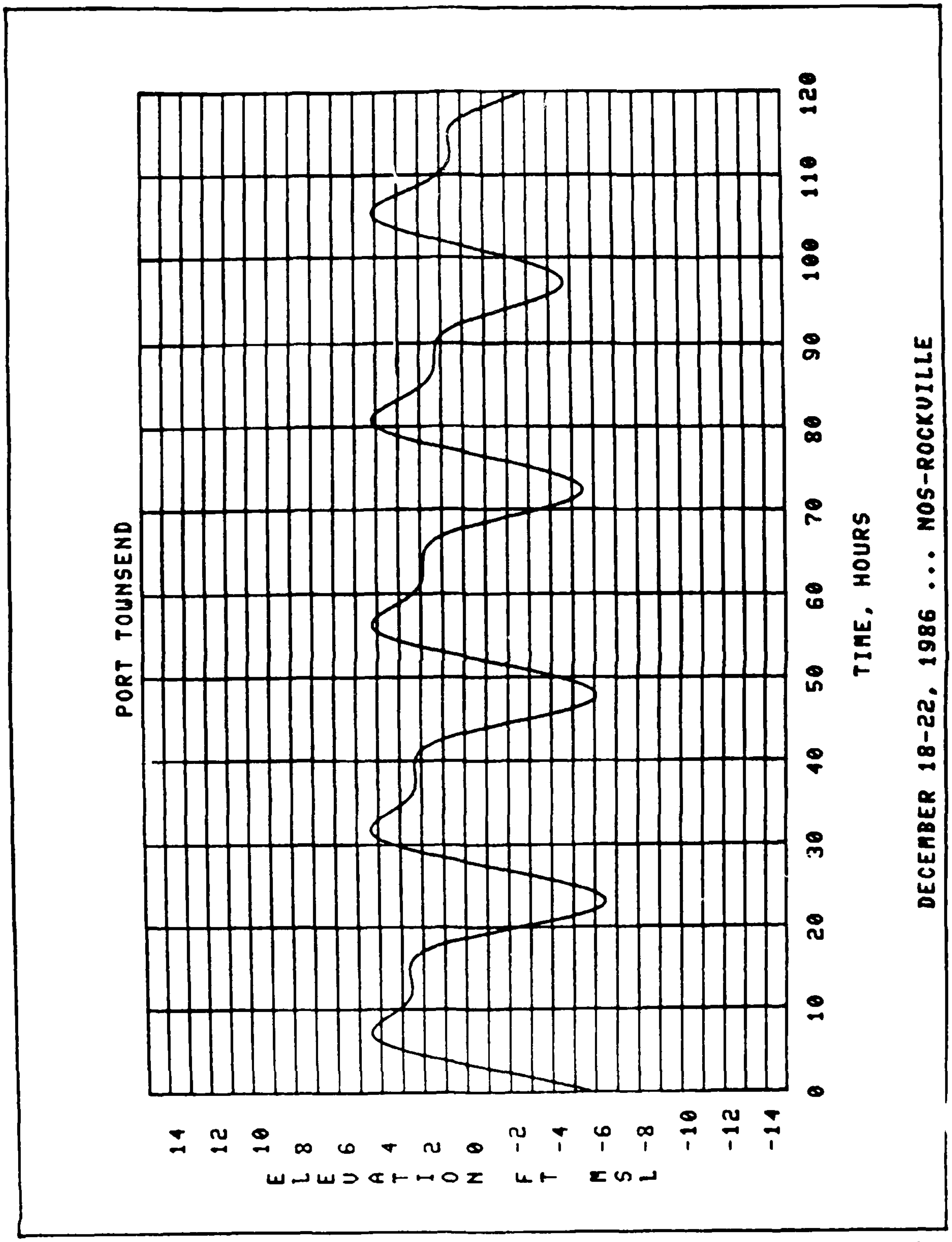

PORT TOWNSEND
ELEVATION FT MSL
14
12
10
8
6
4
2
0
-2
-4
-6
-8
-10
-12
-14
0
10
20
30
40
50
60
70
80
90
100
110
120
TIME, HOURS
DECEMBER 18-22, 1986 ... NOS-ROCKVILLE

PLATE 1

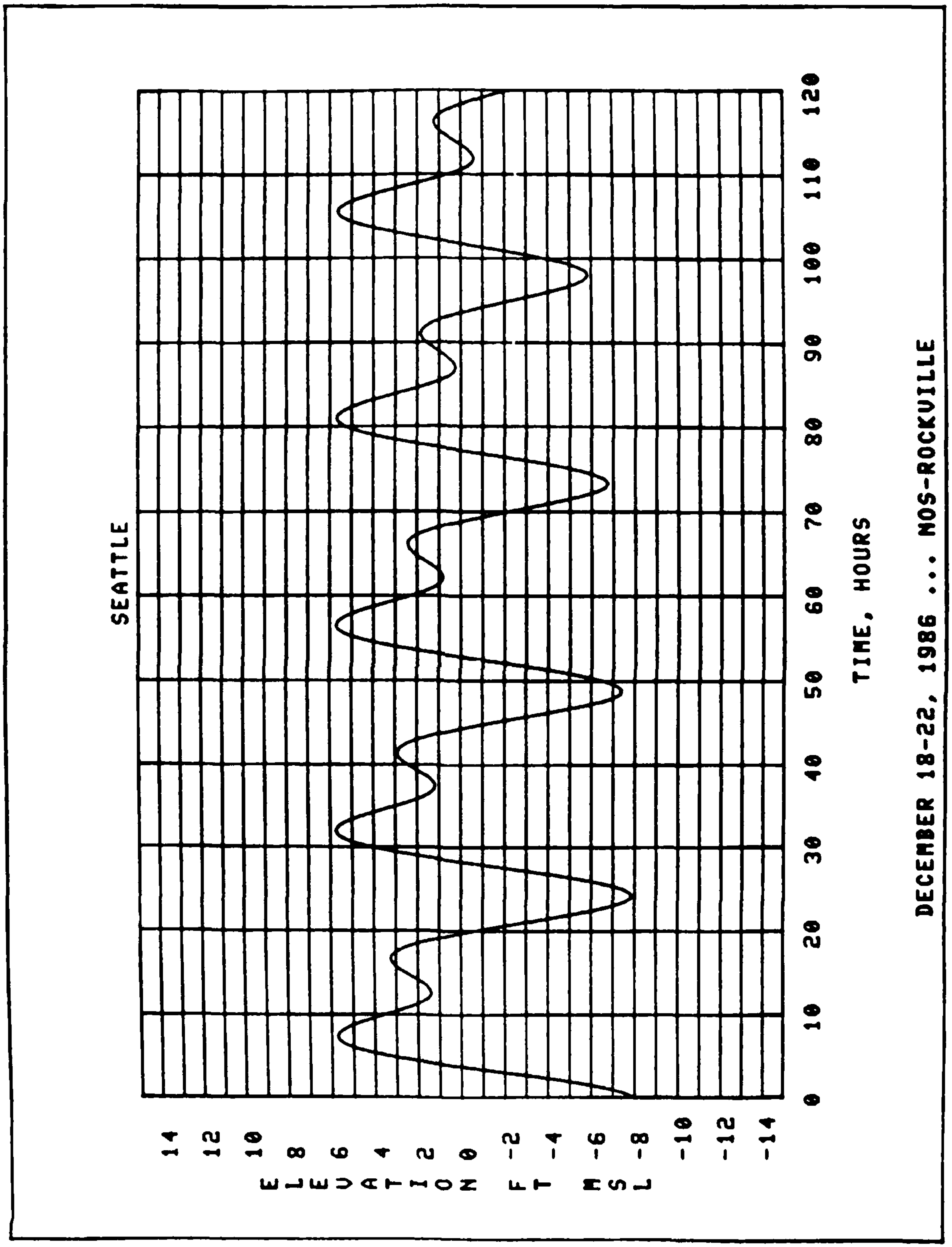
SEATTLE
ELEVATION FT MSL
14
12
10
8
6
4
2
0
-2
-4
-6
-8
-10
-12
-14
0
10
20
30
40
50
60
70
80
90
100
110
120
TIME, HOURS
DECEMBER 18-22, 1986 ... NOS-ROCKVILLE

PLATE 2

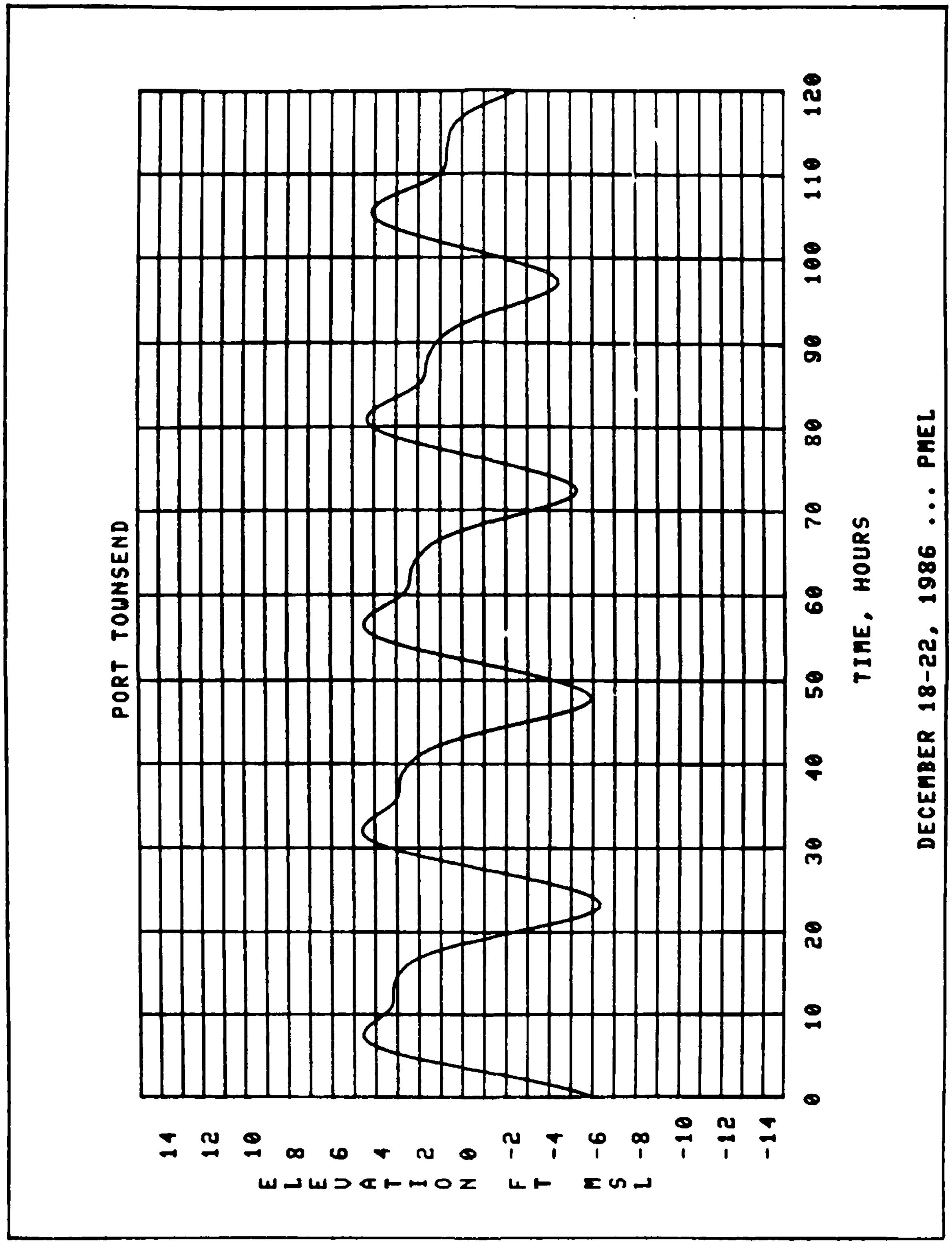
PORT TOWNSEND
ELEVATION FT MSL
14
12
10
8
6
4
2
0
-2
-4
-6
-8
-10
-12
-14
0
10
20
30
40
50
60
70
80
90
100
110
120
TIME, HOURS
DECEMBER 18-22, 1986 ... PMEL

PLATE 3

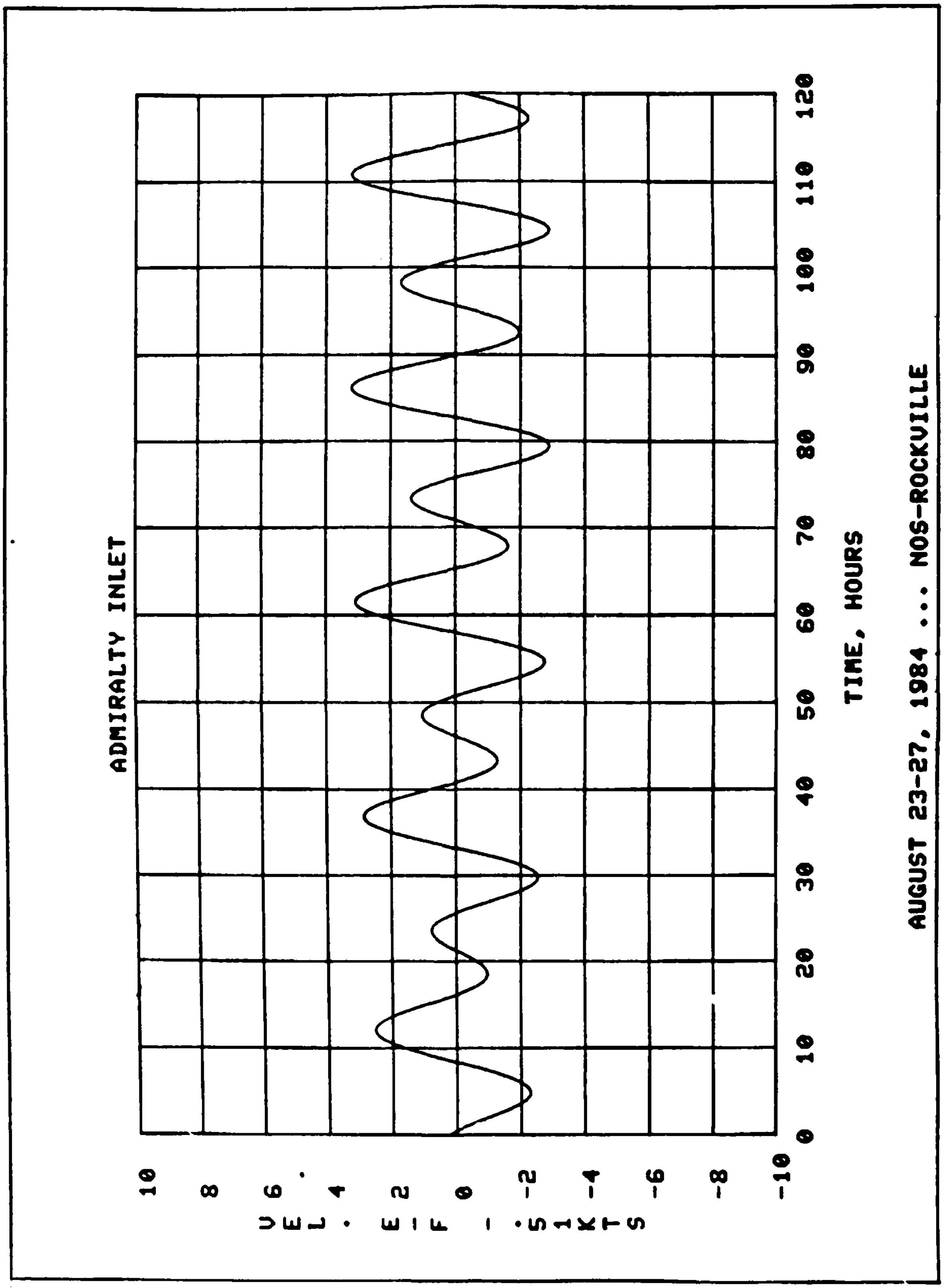
ADMIRALTY INLET
10
8
6
4
2
0
-2
-4
-6
-8
-10
0
10
20
30
40
50
60
70
80
90
100
110
120
TIME, HOURS
AUGUST 23-27, 1984 ... NOS-ROCKVILLE

PLATE 4

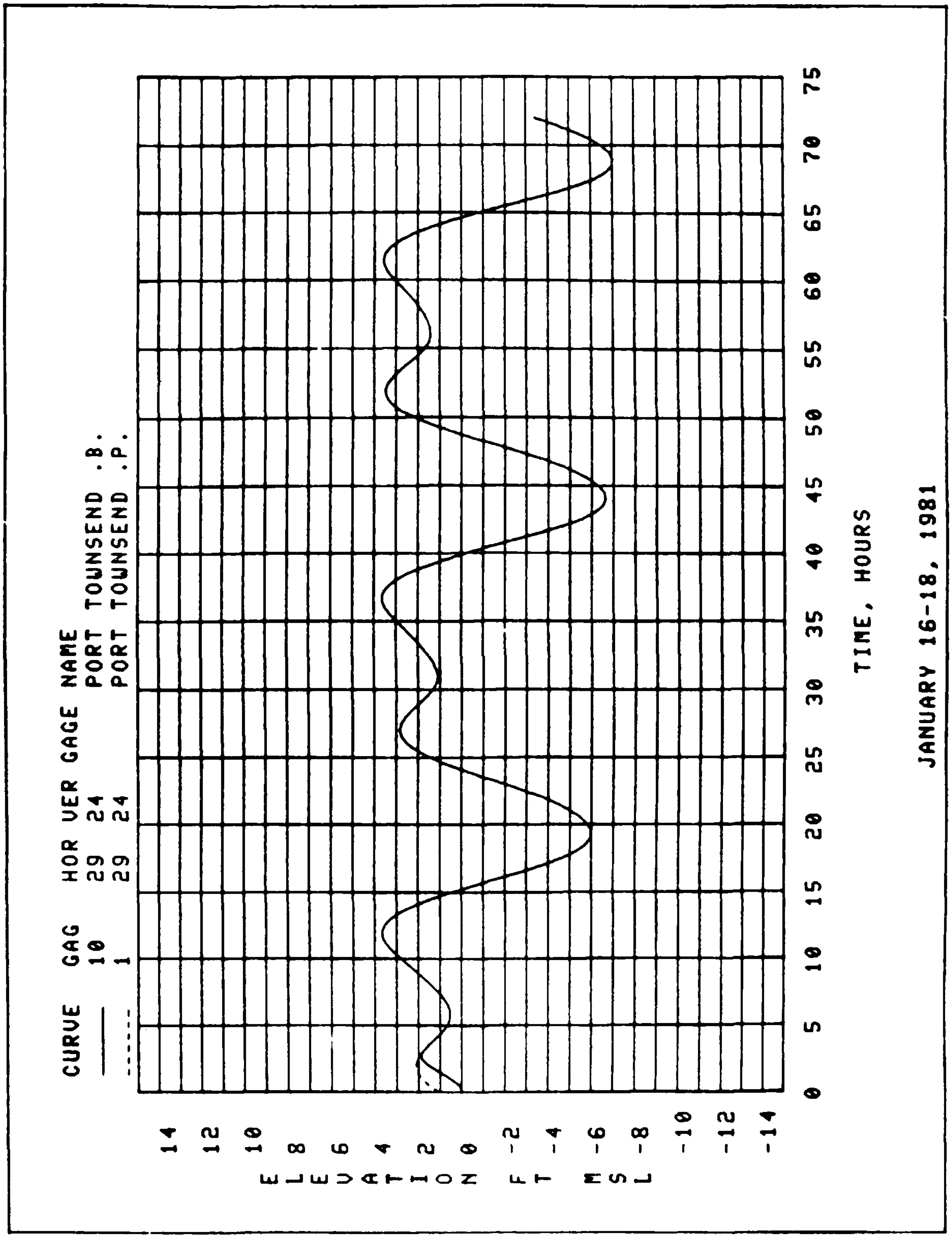
CURVE GAG HOR VER GAGE NAME
10 29 24 PORT TOWNSEND .B.
1 29 24 PORT TOWNSEND .P.
ELEVATION FT MSL
14 12 10 8 6 4 2 0 -2 -4 -6 -8 -10 -12 -14
0 5 10 15 20 25 30 35 40 45 50 55 60 65 70 75
TIME, HOURS
JANUARY 16-18, 1981

PLATE 5

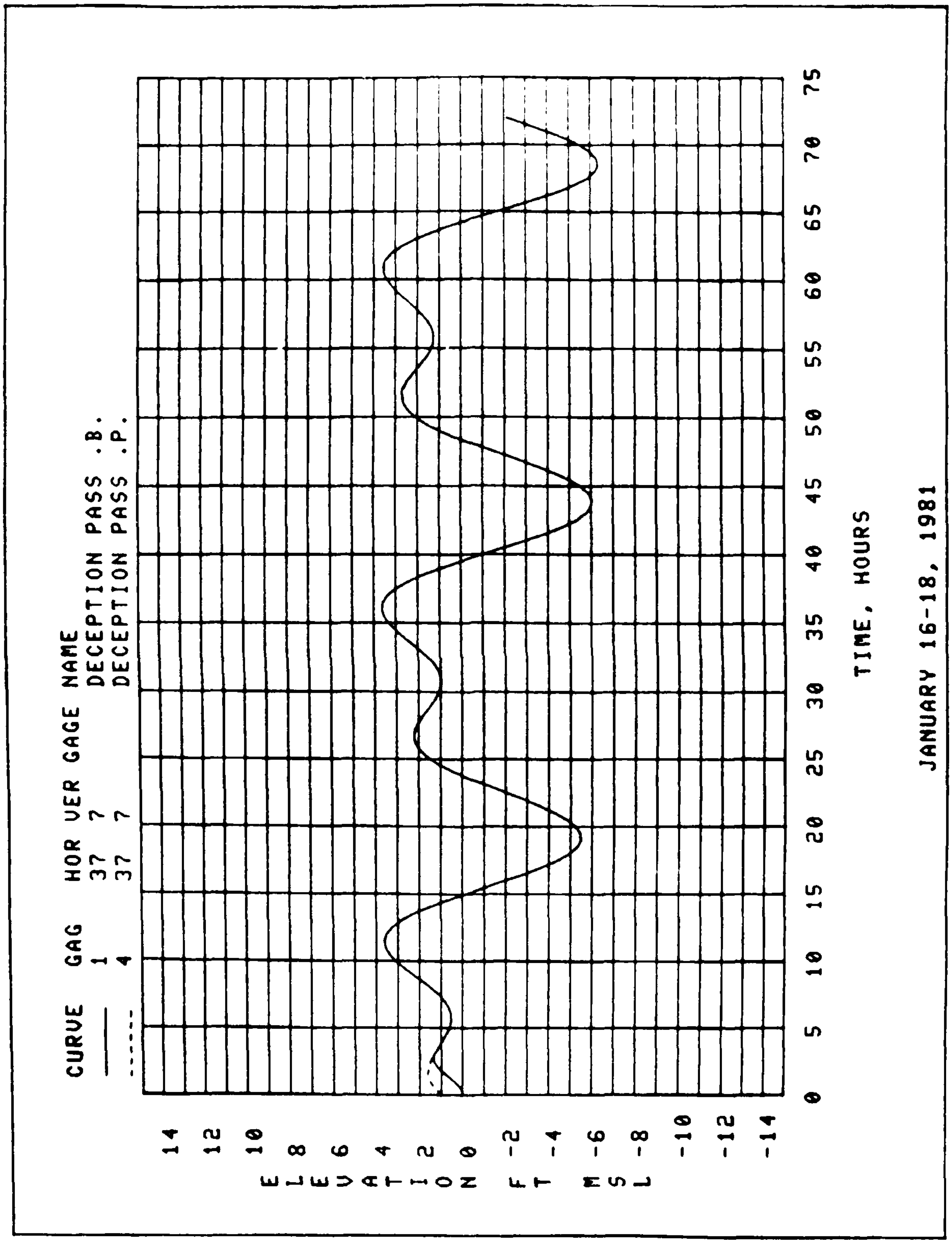
CURVE GAG HOR VER GAGE NAME
1 37 7 DECEPTION PASS .B.
4 37 7 DECEPTION PASS .P.
ELEVATION FT MSL
TIME, HOURS
JANUARY 16-18, 1981

PLATE 6

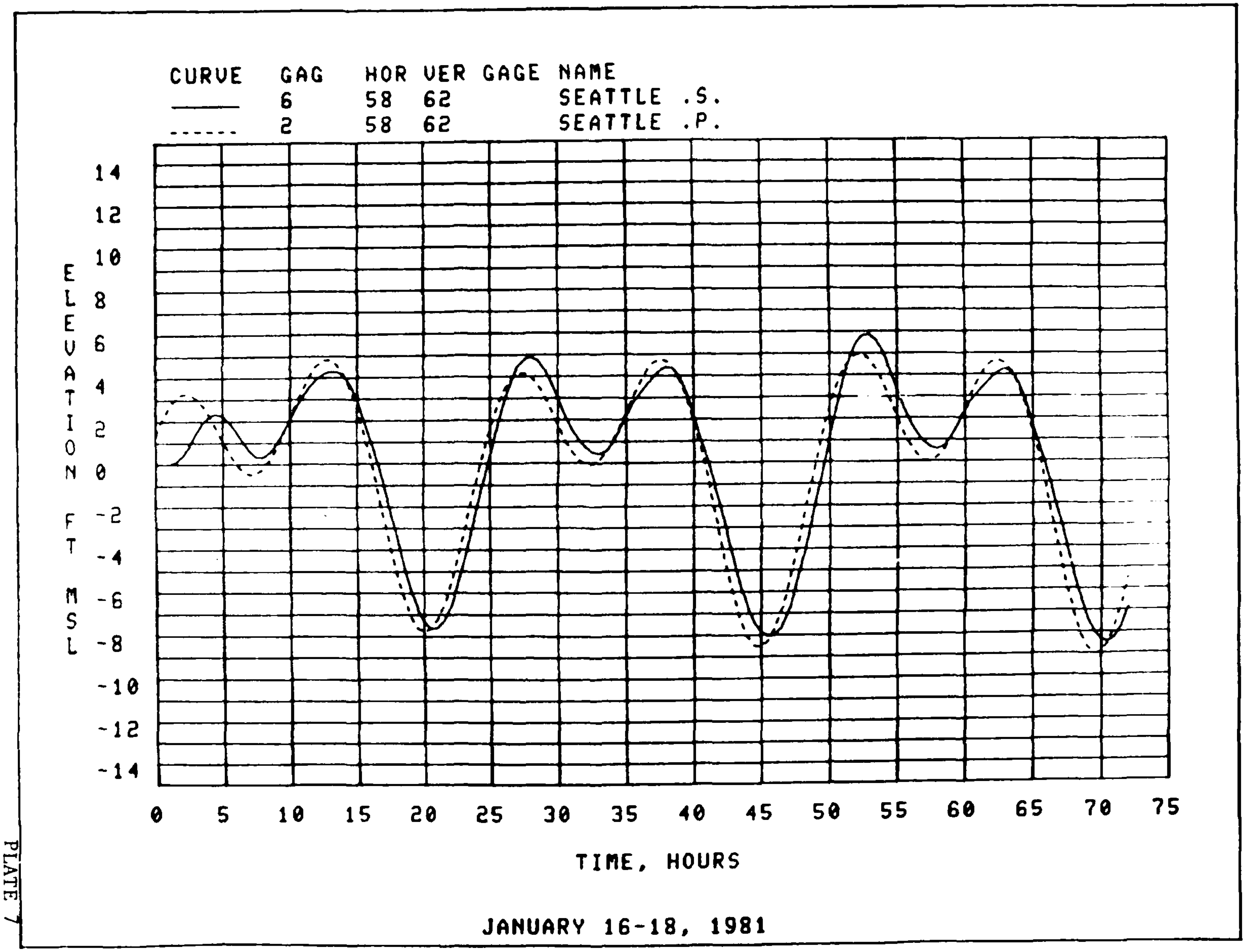

CURVE GAG HOR VER GAGE NAME
6 58 62 SEATTLE .S.
2 58 62 SEATTLE .P.
ELEVATION FT MSL
14
12
10
8
6
4
2
0
-2
-4
-6
-8
-10
-12
-14
0 5 10 15 20 25 30 35 40 45 50 55 60 65 70 75
TIME, HOURS
JANUARY 16-18, 1981

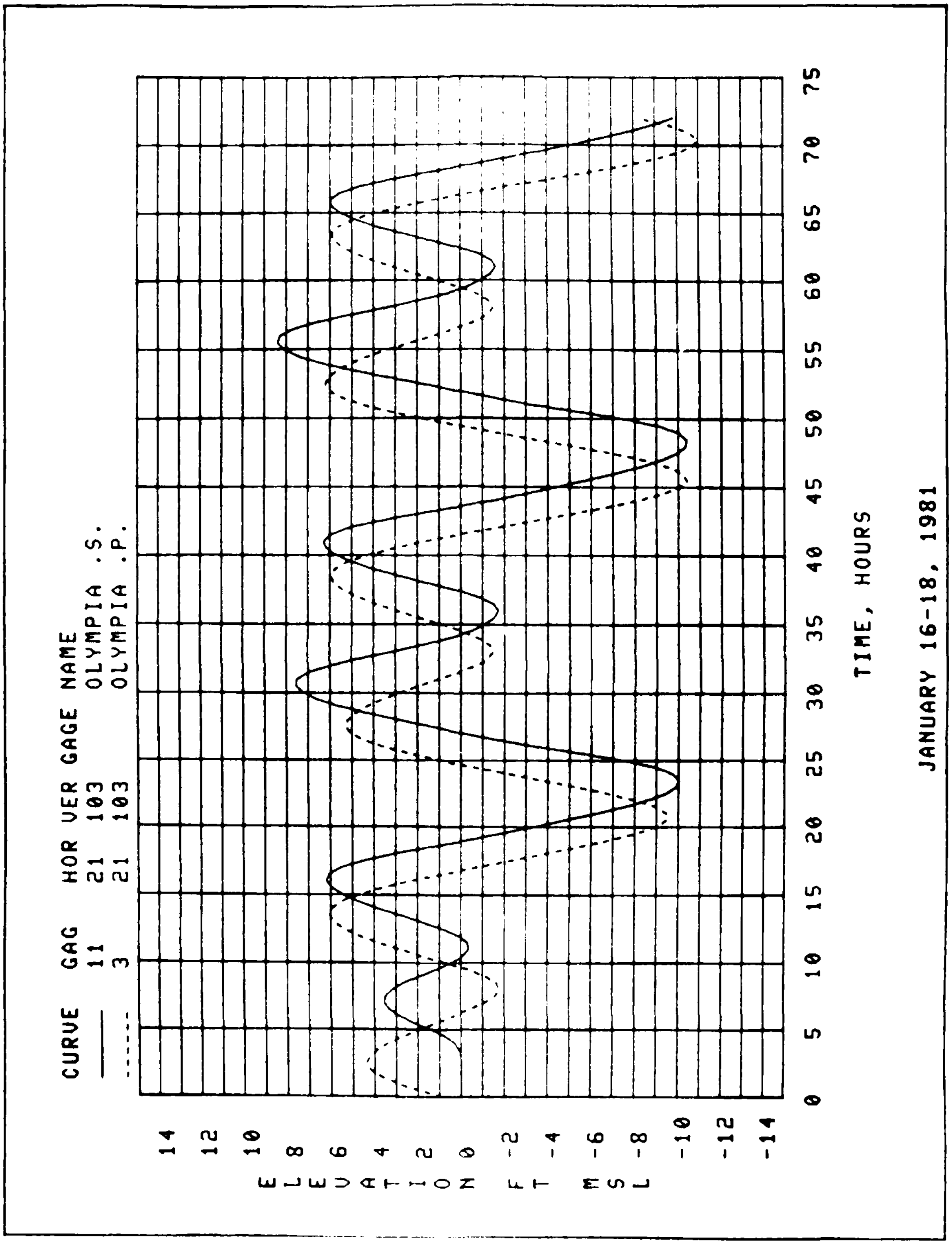
CURVE GAG HOR VER GAGE NAME
11 21 103 OLYMPIA .S.
3 21 103 OLYMPIA .P.
ELEVATION FT MSL
14
12
10
8
6
4
2
0
-2
-4
-6
-8
-10
-12
-14
0 5 10 15 20 25 30 35 40 45 50 55 60 65 70 75
TIME, HOURS
JANUARY 16-18, 1981

PLATE 8

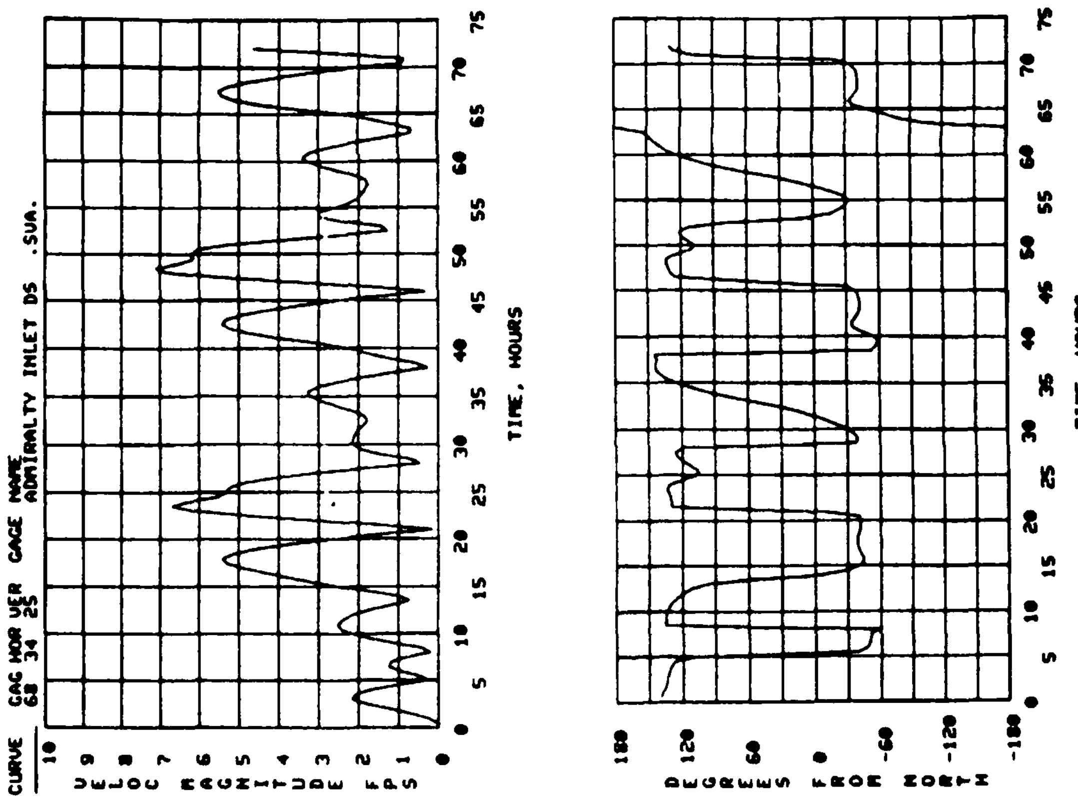

CURVE GAG HOR VER GAGE NAME
68 34 25 ADMIRALTY INLET DS .SVA.
VELOC MAGNITUDE FPS
0 1 2 3 4 5 6 7 8 9 10
0 5 10 15 20 25 30 35 40 45 50 55 60 65 70 75
TIME, HOURS
DEGREES FROM NORTH
-180 -120 -60 0 60 120 180
0 5 10 15 20 25 30 35 40 45 50 55 60 65 70 75
TIME, HOURS
JANUARY 16-18, 1981

PLATE 9

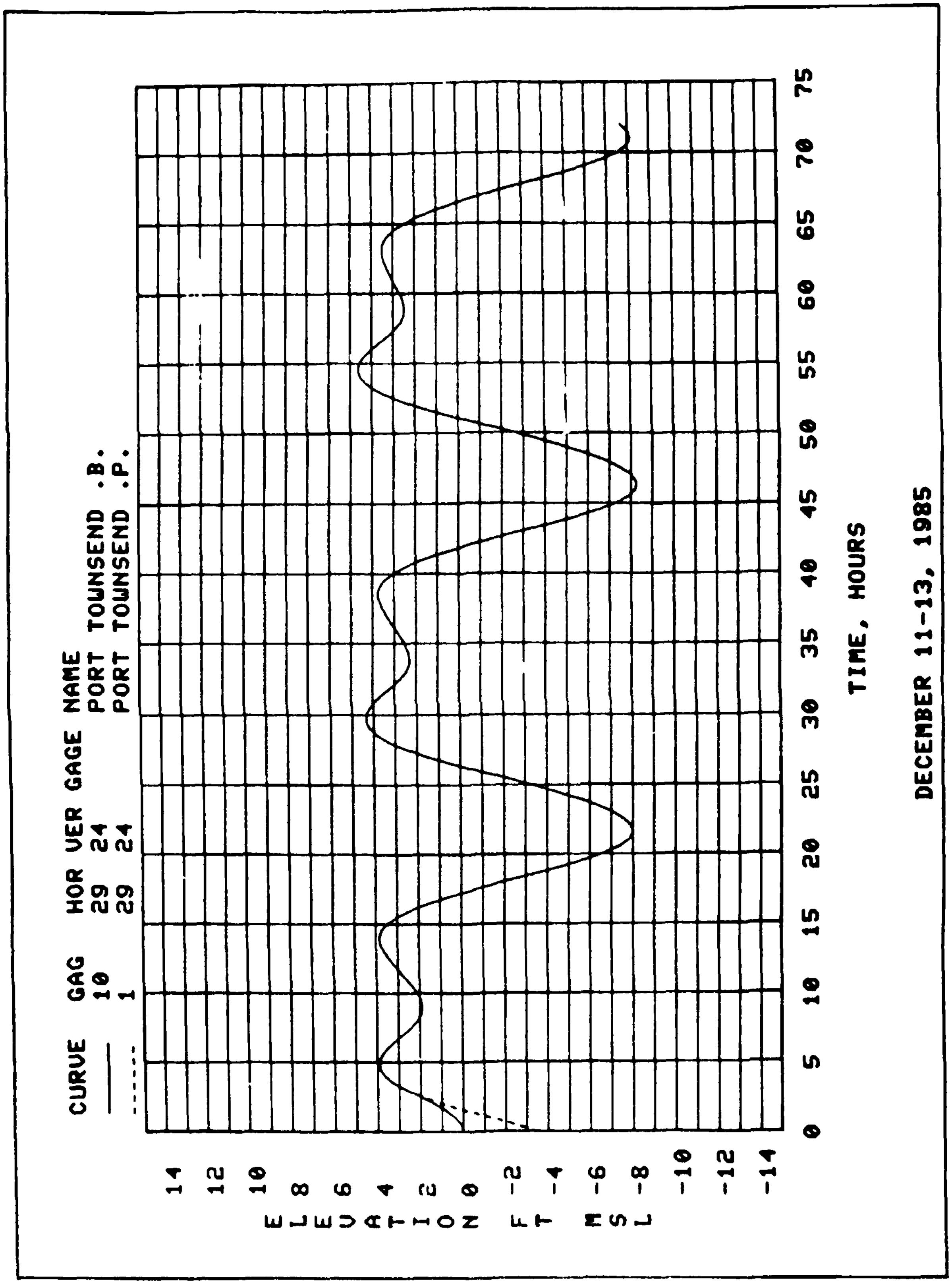
CURVE GAG HOR VER GAGE NAME
10 29 24 PORT TOWNSEND .B.
1 29 24 PORT TOWNSEND .P.
ELEVATION FT MSL
TIME, HOURS
DECEMBER 11-13, 1985

PLATE 10

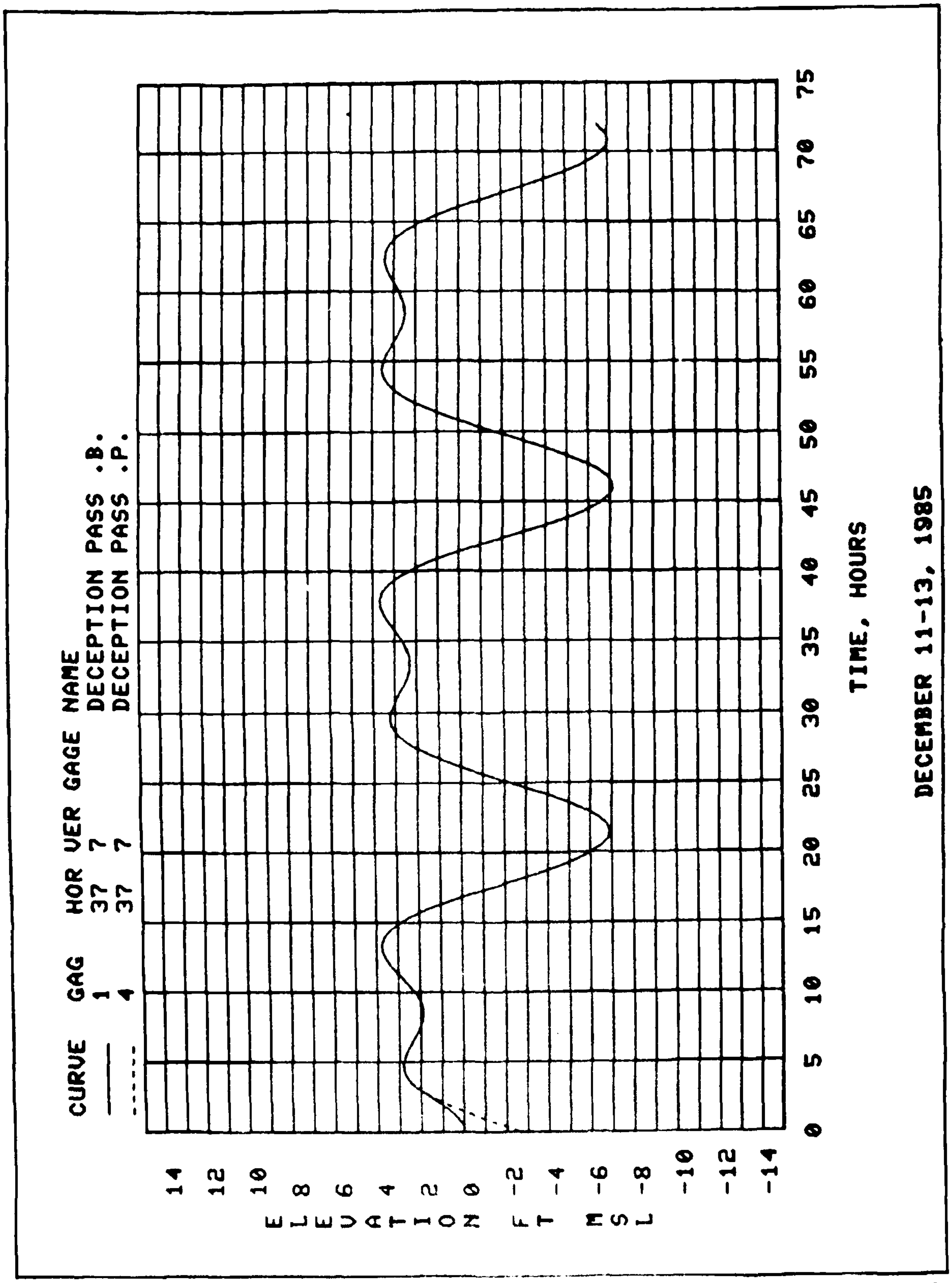
CURVE GAG HOR VER GAGE NAME
1 37 7 DECEPTION PASS .B.
4 37 7 DECEPTION PASS .P.
ELEVATION FT MSL
TIME, HOURS
DECEMBER 11-13, 1985

PLATE 11

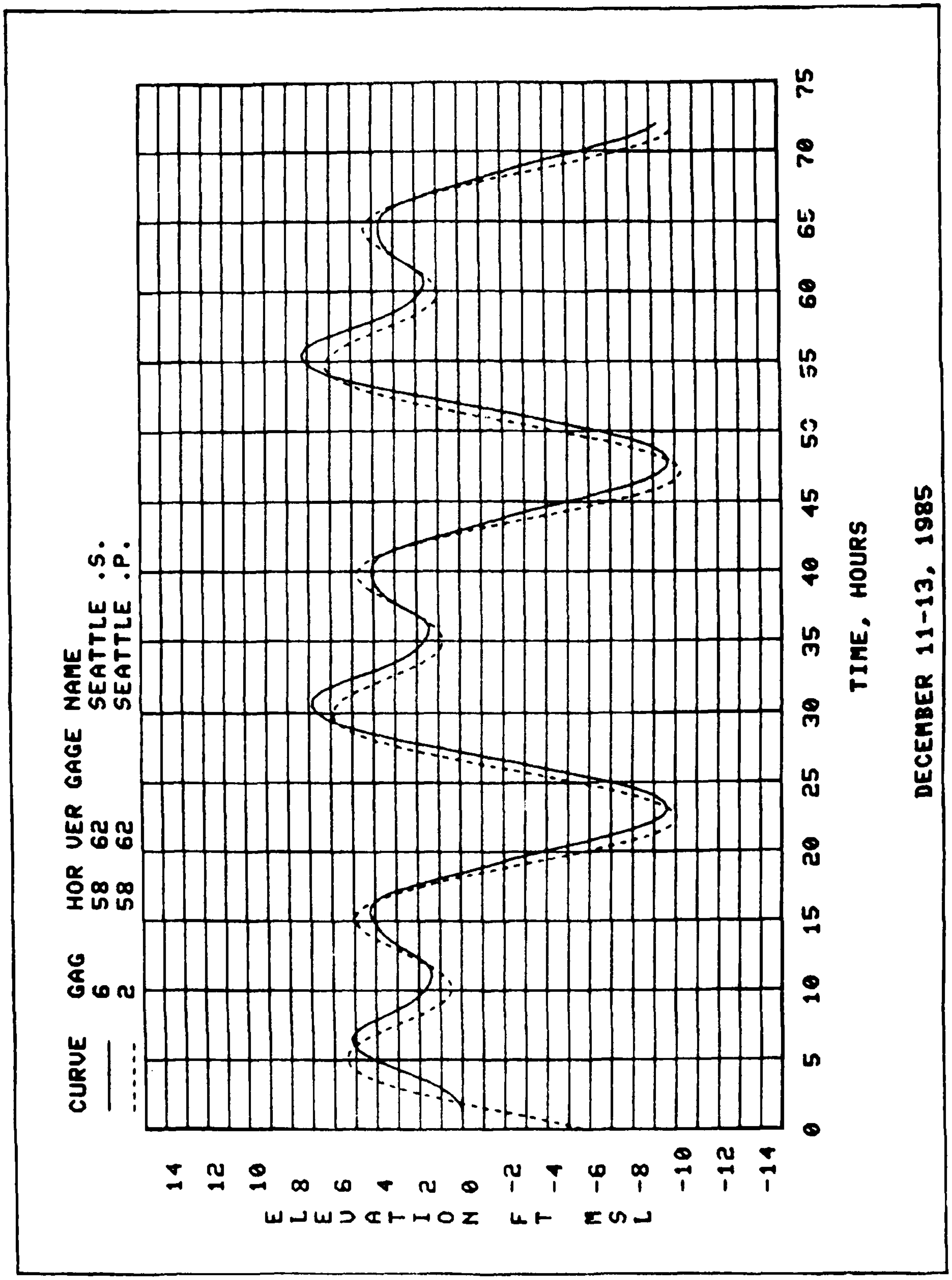
CURVE GAG HOR VER GAGE NAME
6 58 62 SEATTLE .S.
2 58 62 SEATTLE .P.
ELEVATION FT MSL
14 12 10 8 6 4 2 0 -2 -4 -6 -8 -10 -12 -14
0 5 10 15 20 25 30 35 40 45 50 55 60 65 70 75
TIME, HOURS
DECEMBER 11-13, 1985

PLATE 12

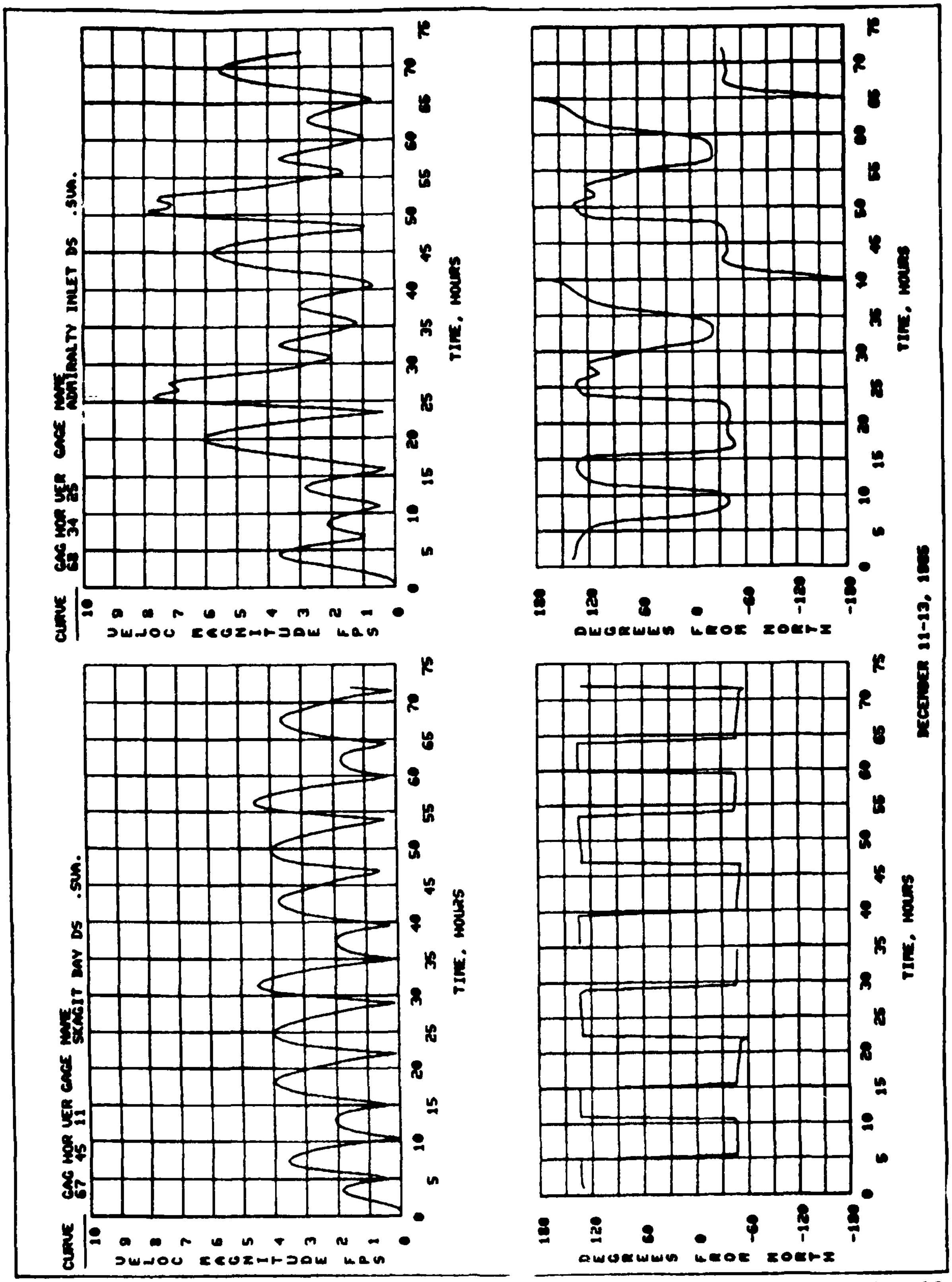

CURVE GAG HOR VER GAGE NAME
68 34 25 ADMIRALTY INLET DS .SVA.
CURVE GAG HOR VER GAGE NAME
67 45 11 SKAGIT BAY DS .SVA.
VELOC MAGNITUDE FPS
DEGREES FROM NORTH
TIME, HOURS
DECEMBER 11-13, 1985

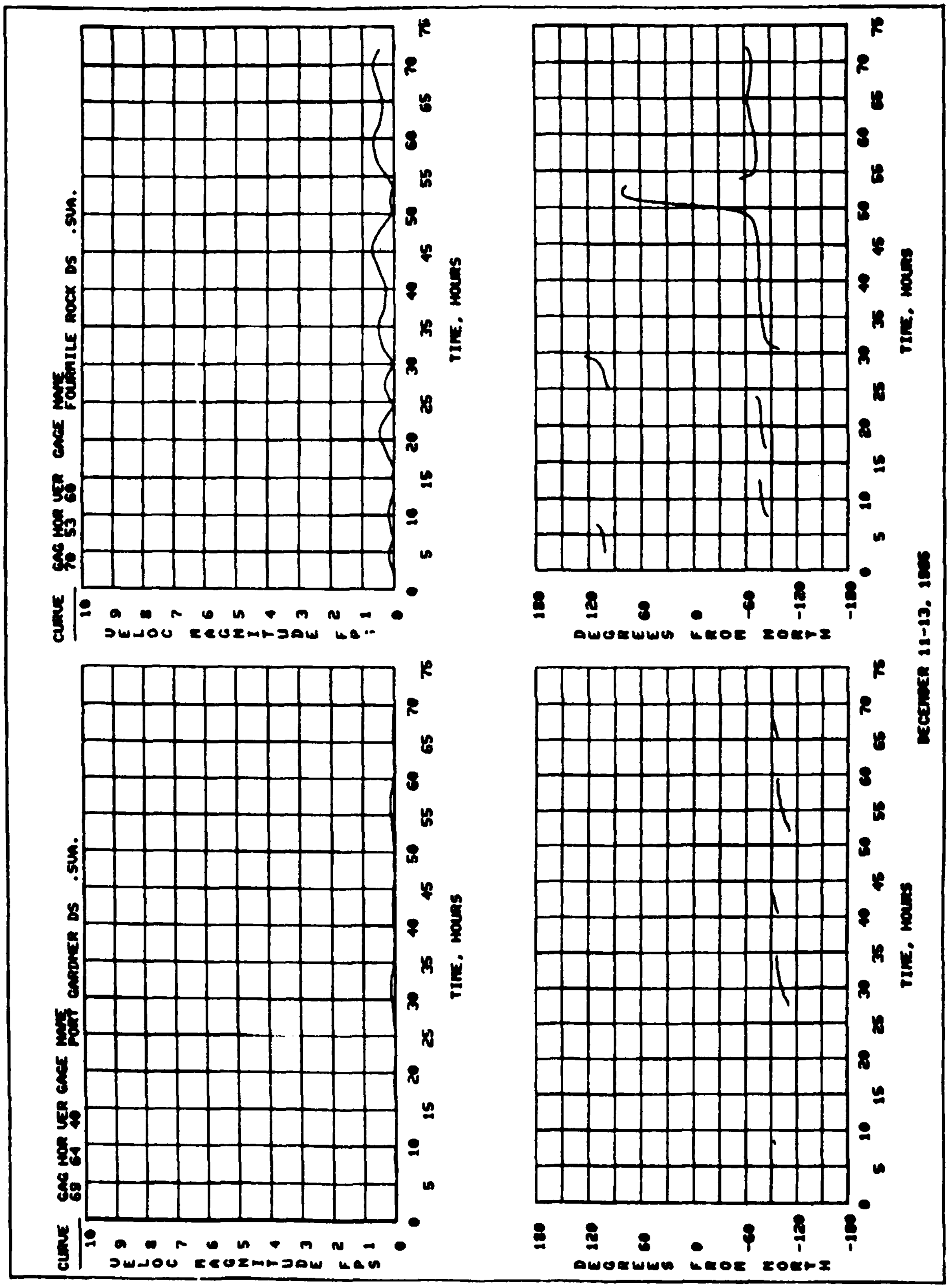
CURVE GAG HOR VER GAGE NAME
10 70 53 60 FOURMILE ROCK DS .SUA.
10 69 64 40 PORT GARDNER DS .SUA.
VELOCITY MAGNITUDE FPS
DEGREES FROM NORTH
TIME, HOURS
DECEMBER 11-13,

PLATE 14

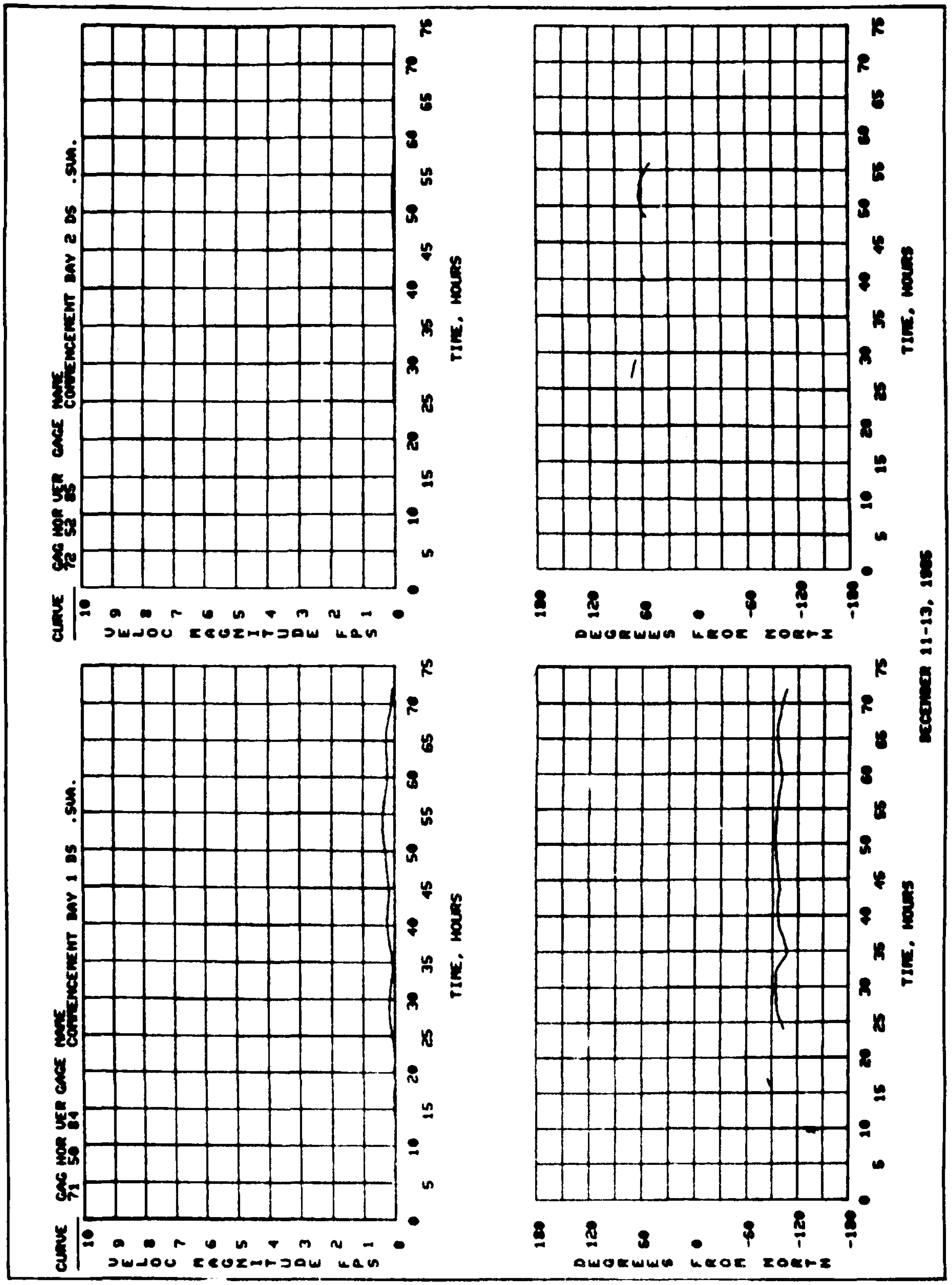
CURVE
GAG HOR VER GAGE NAME
72 52 85 COMMENCEMENT BAY 2 DS .SUA.
TIME, HOURS
DEGREES FROM NORTH
CURVE
GAG HOR VER GAGE NAME
71 50 84 COMMENCEMENT BAY 1 BS .SUA.
TIME, HOURS
DEGREES FROM NORTH
DECEMBER 11-13, 1985

PLATE 15

PLATE 16

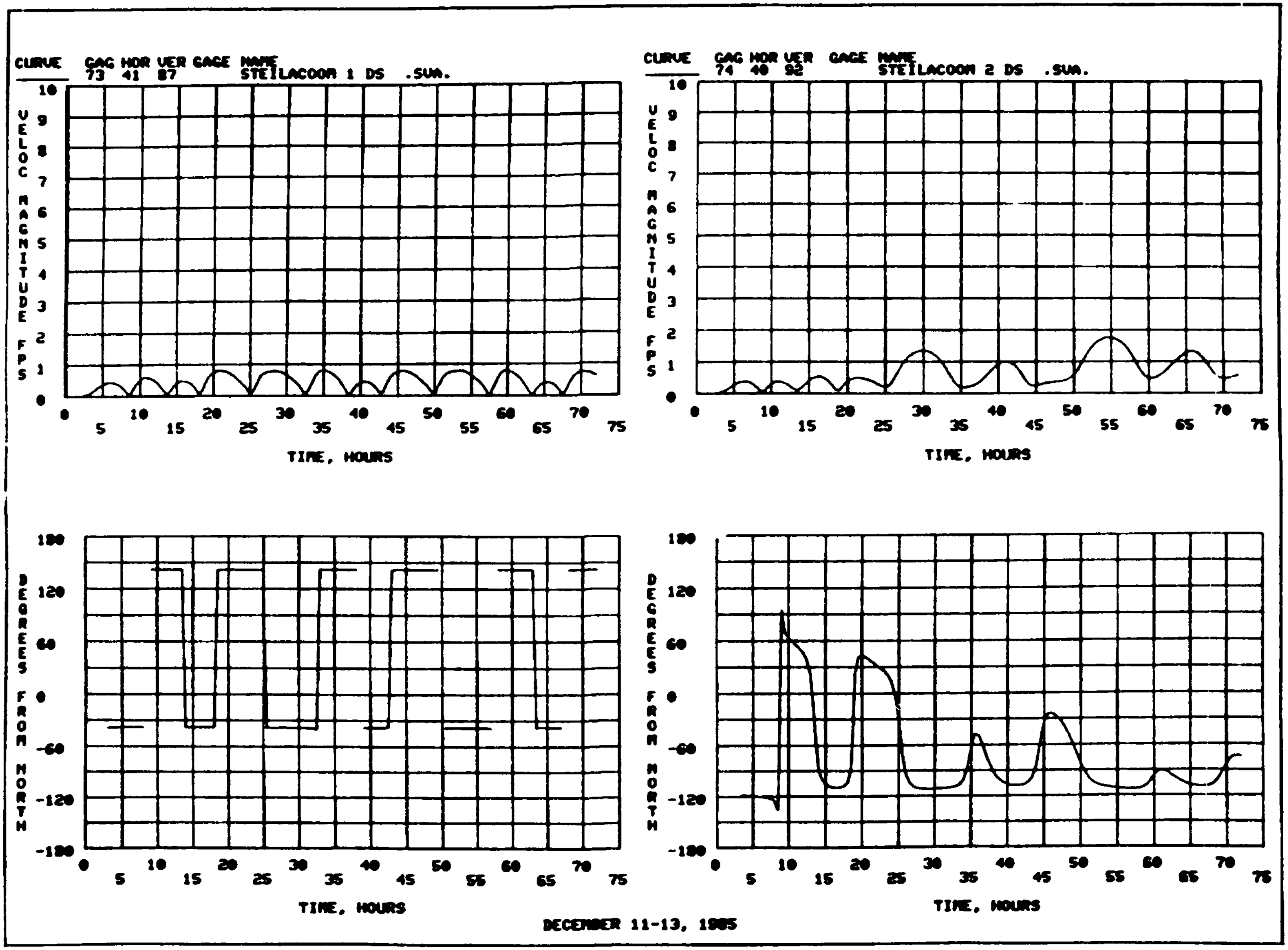

CURVE GAG HOR VER GAGE NAME
73 41 87 STEILACOOM 1 DS .SUM.
CURVE GAG HOR VER GAGE NAME
74 40 92 STEILACOOM 2 DS .SUM.
VELOC MAGNITUDE FPS
DEGREES FROM NORTH
TIME, HOURS
DECEMBER 11-13, 1985

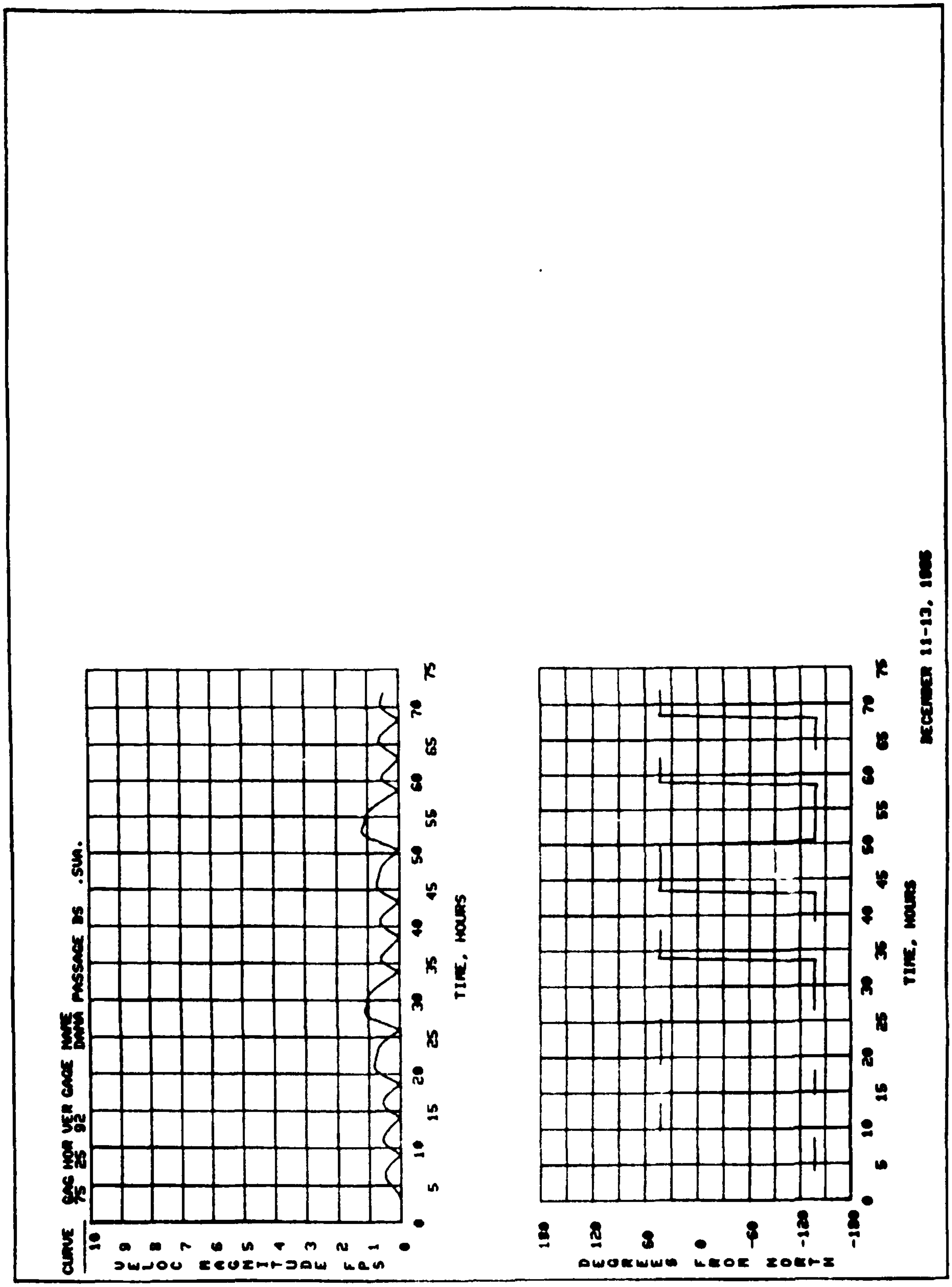
CURVE
GAG HOR VER GAGE NAME
75 25 92 DANA PASSAGE
TIME, HOURS
TIME, HOURS

PLATE 17

END

1-87

DTIC